Received: 2 December 2022 | Revised: 4 January 2023 | Accepted: 5 January 2023

DOI: 10.1002/cjce.24833

SPECIAL ISSUE ARTICLE

THE CANADIAN JOURNAL OF CHEMICAL ENGINEERING

Polyolefin microstructural deconvolution methods: The good, the bad, and the ugly

João B. P. Soares

Department of Chemical and Materials Engineering|, University of Alberta, Edmonton, Alberta, Canada

Correspondence
João B. P. Soares, Department of Chemical and Materials Engineering, University of Alberta, Edmonton, AB, Canada.
Email: jsoares@ualberta.ca

Abstract

The deconvolution of the molecular weight distribution (MWD) of polyolefins into Schultz–Flory most probable distributions has become the standard method to identify the number of site types on multiple-site-type olefin polymerization catalysts such as Ziegler–Natta, Phillips, and some supported metallocenes. This method has been used to quantify the effect of polymerization conditions and catalyst formulations on polyolefin MWD and olefin polymerization kinetics. Related methods have also been developed to deconvolute other polyolefin microstructure features, such as the chemical composition and comonomer sequence length distributions. In this paper, I explain the premises behind these deconvolution models and review the publications in this area, highlighting the advantages, disadvantages, and misuses of these methods. I also propose a revised formulation on how to model the MWD of polyolefins made with multiple-site-type catalysts using ratio distributions for propagation and chain transfer frequencies. The main objective of this overview article is to highlight the strengths, but also show the pitfalls, of polyolefin microstructure deconvolution methods.

KEYWORDS

deconvolution, modelling and simulation studies, polyethylene, polymer characterization, polyolefins, polypropylene

> All homogenous polyolefins are alike, but each heterogeneous polyolefin is heterogeneous in its own way.

1 | EXPLAINING DECONVOLUTION METHODS

You may wonder why deconvolution methods are so common in polyolefin reaction engineering. After all, they are seldom used to model the microstructures of other polymers. I will explain why and pinpoint the good, the bad, and the ugly uses of these methods in this article.

When I started my PhD thesis under the supervision of Archie Hamielec—whom we are honouring in this issue of *The Canadian Journal of Chemical Engineering*—in the early 90s, two explanations for the broad molecular weight distribution (MWD) of Ziegler–Natta polyolefins were facing each other across the theoretical battlefield. The breadth of these distributions was puzzling because

the polymerization mechanism for Ziegler–Natta catalysts predicted that they should make polyolefins with dispersities of two ($Đ = 2$)—as predicted by Schulz-Flory most probable distribution (MPD)[1–5]—not broad MWDs with $Đ > 4$. What, we wondered, was behind this mismatch between polymerization mechanism and polymer microstructure?[6]

One camp argued that concentration and temperature gradients in the polymer particles broadened the MWD. The other camp counterargued that Ziegler–Natta catalysts had different active site types, each making distinct polymer populations; the broad MWD resulted from the overlapping of narrower MWDs, each with the expected $Đ = 2$. Both justifications rested on solid ground for any heterogenous catalyst: chemical engineers quantify mass and heat transfer resistances with the Thiele modulus,[7] while chemists know that heterogenous catalysts have complex surfaces that may give rise to different types of active sites.[8,9] (I took pains to specify the distinction between chemical engineers and chemists here because this was vaguely how the lines were drawn at that time.)

If a heterogenous catalyst makes small molecules—ammonia, for instance—these effects don't matter as much: even though different site types and radial gradients may affect catalyst productivity and selectivity, every ammonia molecule still looks and behaves alike. But they become relevant for polymers because the effects of particle gradients and different site types are engraved into the microstructure of the polymer chains. The microstructure and properties of a polyolefin made under mass and heat transfer resistances with a multiple-site-type catalyst differ from those of a polyolefin made without transport limitations with a single-site-type catalyst, even if they are made in the same reactor under the same polymerization conditions. The academic consequences are stimulating—we must look for answers to so many fundamental questions about these polymerization process—but the industrial consequences are a matter of make it or break it in the competitive polyolefin market.

Like in most conflicts, both sides had valid points. These explanations are not mutually exclusive. We know today that not only Ziegler–Natta and other heterogeneous coordination catalysts have more than one active site type but also that they may also be subject to radial concentration and temperature gradients during polymerization. Site multiplicity is the main cause of broad MWDs, but particle gradients may broaden these distributions even more. Intraparticle mass and heat transfer resistances are a fascinating topic of research; however, they are not the main reason why polyolefins made with Ziegler–Natta catalysts have broad MWDs. I won't spend much time talking about them in this article. If you are interested in this topic, take a look at my recent review paper with Tim McKenna,[10] which gives a bird's eye view on this subject.

MWD deconvolution ignores radial gradients—as well as other positional and temporal gradients, as I will explain later—and assumes that different site types cause the broad MWDs of polyolefins made with heterogeneous coordination catalysts (Ziegler–Natta, Phillips, and some supported metallocenes and post-metallocenes). Can you ignore radial, positional, and temporal gradients? It depends on the conditions of your polymerizations. If you use the deconvolution procedure with data collected under the right conditions, you will estimate consistent values for your models, from laboratory to industrial scale (the good). If you don't, then all bets are off (the bad or the ugly). Like in any modelling procedure, the implacable garbage in, garbage out (GIGO) paradigm dictates the outcomes of the deconvolution process.

Archie and I popularized MWD deconvolution methods, but we didn't discover them. Deconvolution methods had already been used for a while to analyze peaks in other chromatographic and spectrographic methods.[11–19] Vickroy et al.[20] reviewed previous models for the MWD of polyolefins and proposed a simple method to deconvolute the MWD of high density polyethylene (HDPE) into Flory distributions. (Flory and Schulz derived the most probable distribution independently at about the same time. Even though it's more proper to call it the Schulz-Flory distribution, I will opt for the shorter denomination, Flory distribution, in this paper.) At the time, I was developing a mathematical model to quantify intraparticle mass and heat transfer resistances in multiple-site-type catalysts using the method of moments. Archie showed me Vickroy et al.'s paper and suggested that I could use their more elegant method in my model. (Those who knew Archie will remember his passion for elegant solutions.) He also suggested that if I replaced Flory most probable distribution with Stockmayer bivariate distribution,[21] I could predict the joint molecular weight and chemical composition distribution (CCD) (MWD × CCD) of ethylene/propylene/1-olefin copolymers. (Incidentally, Archie met these great men, Paul Flory and Walter Stockmayer. One of the pleasures of working for Archie was that he knew everyone in the field.)

This was a brilliant insight. I am still thankful that I followed Archie's advice. We published a modelling paper—which didn't include a deconvolution method, just a new approach to describe the joint MWD × CCD of copolymers made with a heterogeneous multiple-site-type catalyst under mass and heat transfer limitations—in 1995.[6] In the same year, we wrote two other papers using this concept, one on how to use Stockmayer distribution to model temperature rising elution fraction (TREF),[22] and the other on how to systematically deconvolute broad MWDs into a series of Flory distributions.[23] It's worth reviewing our deconvolution assumptions here, since the method won't produce reliable results if they are violated[23]:

1. The polymer is made in a reactor operated at steady state.
2. The reactor conditions are spatially uniform.
3. The ratio of chain transfer to propagation rates doesn't change during the polymerization.
4. Intraparticle mass and heat transfer resistances are negligible.
5. Gel permeation chromatography (GPC) must measure the actual MWD of the polymer.

The first four assumptions are tied to the same requirement: the polymerization conditions should be such that the polymer made on each site type follows the same Flory distribution at any time and location—inside or outside the polymer/catalyst particle—during the polymerization. The fifth condition states that GPC must measure the actual polymer MWD, without artefacts introduced by axial dispersion or other analytical errors. The first four assumptions fall within the domain of polyolefin reaction engineering; I will discuss their implications in more detail below. The last assumption is a gross error in polymer analysis: without reliable GPC data, any MWD deconvolution method will fail. Precise GPC measurements are sine qua non conditions for MWD deconvolution.

Let's examine the reasons behind these requirements. Flory distribution depends on a single parameter, τ. We should be thankful for this; it's a rare instance of nature helping us, mathematical modellers, as I will explain below.

In log scale, the mass-based Flory distribution, $w_{\log M_r}$, is given by the following equation:

$$w_{\log M_r} = \lambda \left(\frac{M_r}{\overline{M}}\right)^2 \tau^2 \exp\left(-\frac{M_r}{\overline{M}}\tau\right) \tag{1}$$

where λ is a normalization constant ($\lambda = 1/\log e$), M_r is the molecular weight of a chain having r monomeric units, and $\overline{M}$ is the average molar mass of the repeating unit. The parameter τ is the ratio between the sum of all chain transfer frequencies (β-hydride elimination, transfer to hydrogen, transfer to monomer, etc.) and the propagation frequency:

$$\tau = \frac{\sum f_{t_i}}{f_p} \tag{2}$$

The parameter τ is usually defined as the ratio of chain transfer to propagation rates,[23] but lately I have found that defining it as a ratio of frequencies has a few advantages. I explain why in Appendix A.

Equation (1) teaches us that a single parameter, τ, defines the whole MWD of polyolefins made with single-site-type catalysts. Take a moment to let this sink in and to realize the wealth of microstructural information that τ encapsulates. From Equation (1), we also learn that $M_n = \overline{M}/\tau$, $M_w = 2\overline{M}/\tau$, and $Đ = M_w/M_n = 2$. If you change the temperature, pressure, concentrations of monomer, comonomer, or hydrogen, you trigger a cascade of effects: f_{t_i} and f_p change, altering τ, which drags the whole MWD with it.

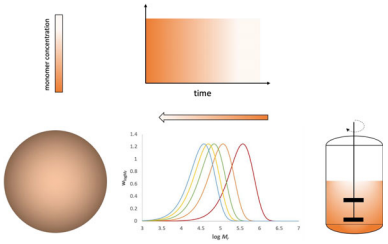

FIGURE 1 The molecular weight distribution (MWD) of a polyolefin made with a single-site-type catalyst will change if the polymerizations conditions vary in time, reactor location, or polymer particle radial position.

Allow me to illustrate why assumptions 1 to 4 above must be obeyed for MWD deconvolution to work. When I parodied Tolstoy and said that 'All homogeneous polyolefins are alike', what I meant to say was that instantaneously all of them have $Đ = 2$ and that, for copolymers, the average comonomer fraction is independent of molecular weight.[10] The qualification instantaneously means that we are describing the properties of polymer populations made at a moment in time—a snapshot, if you are fond of photographic analogies (I am, so bear with me). If the polymerization conditions remain constant in time and space, then the MWD (as well as all other microstructural distributions) never changes, and the instantaneous and cumulative distributions are the same. But if the conditions change, then the instantaneous distributions will drift. Figure 1 illustrates this concept for MWD when the monomer concentration varies inside the particle, within the reactor, or as a function of time.

When we deconvolute the MWD of a polyolefin made with a multiple-site-type catalyst, we assume that the distributions assigned to each site type remain the same throughout the polymerization. If this condition is violated, the MWDs of the polymer populations made on each site type shift during the polymerization, further broadening the MWD. Figure 2 illustrates this effect. If we deconvolute the MWD of a polymer made under non-uniform conditions, we will identify more site types than the minimum required to describe the catalyst. A single-site-type catalyst made the polymer with the MWD on the left of Figure 2. The dashed lines show how the Flory distributions varied during the polymerization, and the red line is the overall (cumulative) MWD. The Flory

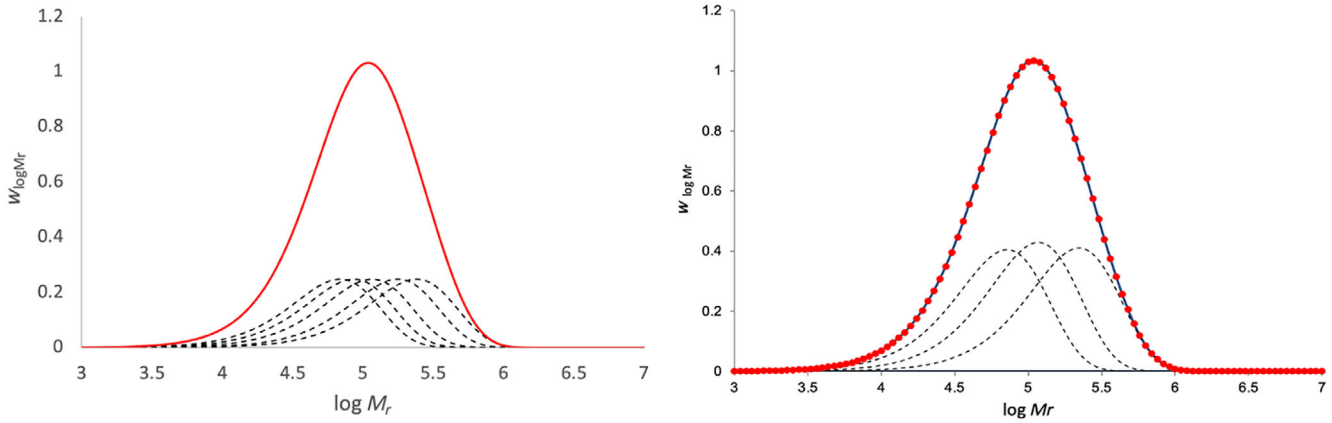

FIGURE 2 The molecular weight distribution (MWD) deconvolution procedure assumes that the only cause of MWD broadening is the presence of more than one active site type. Any other broadening effect will be mistakenly detected as additional active site types.

distributions drifted because the polymerization conditions changed. A deconvolution algorithm would erroneously interpret this MWD (shown as red dots in the plot on the right side of Figure 2) as being made with a catalyst with three different site types (dashed lines). GPC peak broadening would have the same negative effect on deconvolution.

In conclusion, deconvolution only works if no other factors broaden the MWD. Neglecting this requirement will lead to some of the ugly applications of this method. On the positive side, we are lucky that the Flory distribution is the fundamental equation for the MWD of linear coordination polyolefins. Unlike the normal distribution, which is defined by a mean and a standard deviation, Flory's is determined only by its mean ($M_n = \overline{M}/\tau$) and has a fixed standard deviation, $\sigma = M_n\sqrt{M_w/M_n - 1} = M_n$. Why is this important? Figure 3 explains why. Deconvolution methods use non-linear least squares algorithms to minimize the square of the differences between the measured and predicted MWDs:

$$\text{Min}\left(W_{\log M_r}{}^{\exp} - \sum_{i=1}^{n} m_i w_{\log M_r,i}\right)^2 \tag{3}$$

where $W^{\exp}_{\log M_r}$ is the experimental MWD, n is the number of site types, m_i is the mass fraction of polymer made by site type i, and $w_{\log M_r,i}$ is Flory distribution for site type i.

Using Flory distributions, the algorithm can only:

1. Shift peak positions: M_{n_i} or τ_i
2. Change peak areas (polymer population mass fraction): m_i

Let's now compare a similar procedure using normal distributions to describe the populations made on each site type. Now, the algorithm must:

1. Shift peak positions: M_{n_i} or τ_i
2. Change peak areas (polymer population mass fraction): m_i
3. Broaden or narrow the peaks: σ_i

It is the third action above that causes headaches. Finding unique solutions with Flory distributions is easier because they have fixed standard deviations: $\sigma_i = M_{n_i}$. Using normal distributions adds the additional parameter σ and invites multiple solutions: Similar fits can be found with a few broader or many narrower distributions (Figure 3A). But, more importantly, the polymerization mechanism calls for Flory distribution: using the normal—or any other statistical distribution—is just an arbitrary way to fit the MWD. It won't help us understand the fundaments of olefin polymerization with coordination catalysts.

Hamielec and I wondered whether the MWD deconvolution concept could be extended to explain why the CCD of polyolefins made with heterogeneous catalysts was broad for high-density polyethylene (HDPE), and often bimodal for linear low-density polyethylene (LLDPE). In this case, we need to use the CCD component of Stockmayer distribution[22]:

$$w_{F_1} = \frac{3}{4\sqrt{2\beta\tau}}\left[1 + \frac{\left(F_1 - \overline{F}_1\right)^2}{2\beta\tau}\right]^{-5/2} \tag{4}$$

The parameter β in Equation (4) is defined as

$$\beta = \overline{F}_1\left(1 - \overline{F}_1\right)\sqrt{1 - 4\overline{F}_1\left(1 - \overline{F}_1\right)\left(1 - r_1 r_2\right)} \tag{5}$$

where r_1 and r_2 are the reactivity ratios for monomer 1 (ethylene) and 2 (1-olefin), respectively.

In Equation (4), the variable F_1 is the molar fraction of ethylene in a copolymer chain, and $\overline{F}_1$ is the average

THE CANADIAN JOURNAL OF CHEMICAL ENGINEERING

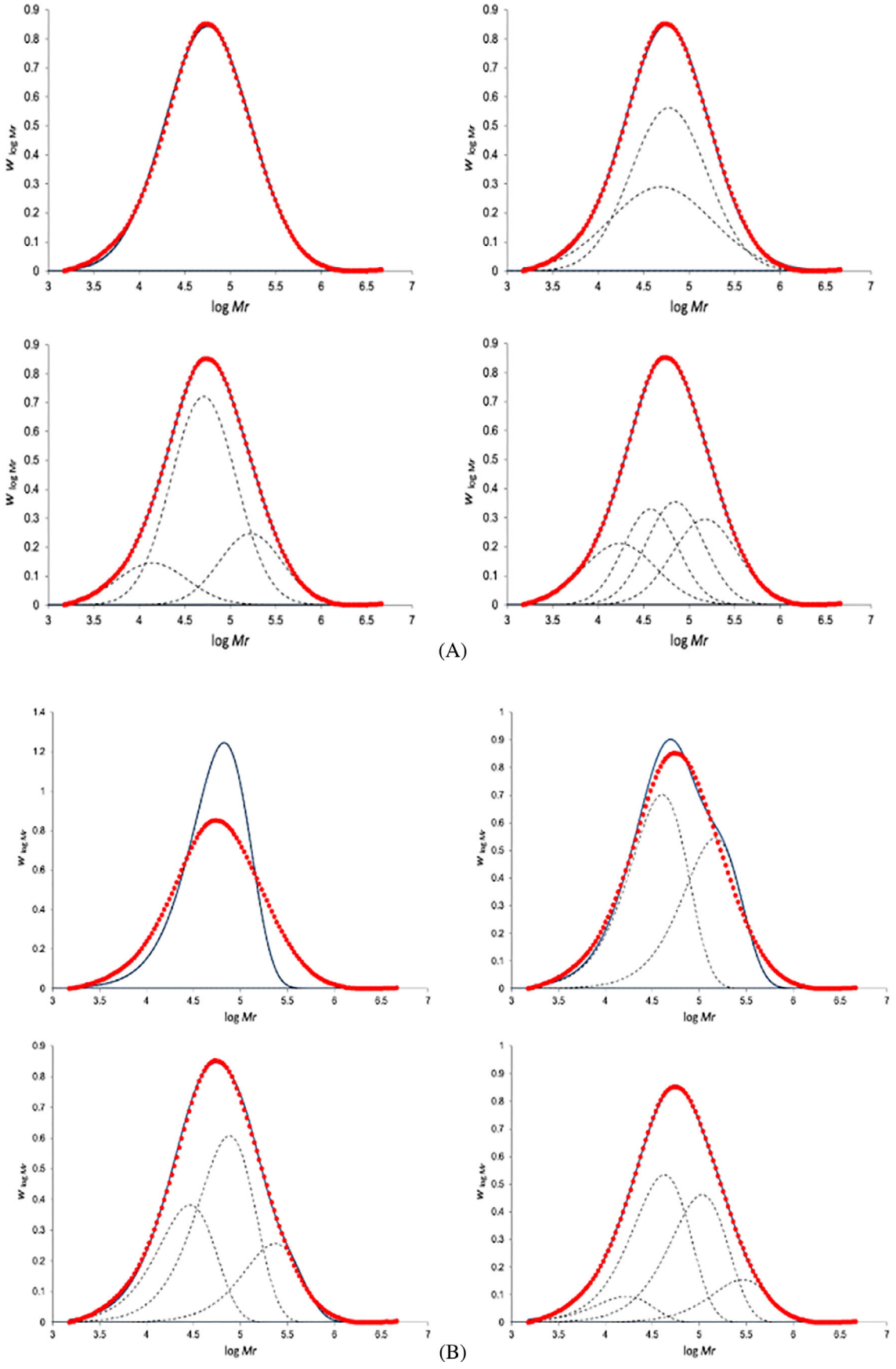

FIGURE 3 Molecular weight distribution (MWD) deconvolution with: (A) normal distributions and (B) Flory distributions. Multiple solutions are more likely with normal (or other) distributions.

molar fraction of ethylene in the copolymer population. Don't get these definitions mixed up: F_1 is the molar fraction of ethylene of a copolymer chain in the population, while $\overline{F}_1$ is the instantaneous average molar fraction of ethylene in the entire copolymer population. The variable F_1 is like the variable M_r in Flory distribution, while the parameter $\overline{F}_1$ is like the parameter M_n.

Figure 4 shows how a bimodal CCD can be described as a superposition of Stockmayer distributions assigned to four catalyst site types.

You may think, as I did, that the next step was to deconvolute the CCD of heterogeneous ethylene/α-olefin copolymers into several Stockmayer CCD components. If we make the same assumptions—no temporal or spatial changes in polymerization conditions—CCD deconvolution should work as well as MWD deconvolution, right? No. It's not so easy. Here is the catch: When GPC is properly operated, it measures the actual MWD of polyolefins, but no analytical method can measure their actual CCD. This statement might surprise you if you have read some of my articles on this topic, because this is exactly what I did: I deconvoluted the CCD of polyolefins made with Ziegler–Natta catalysts into several Stockmayer CCD components. Before you accuse me of being inconsistent, allow me to justify my past work.

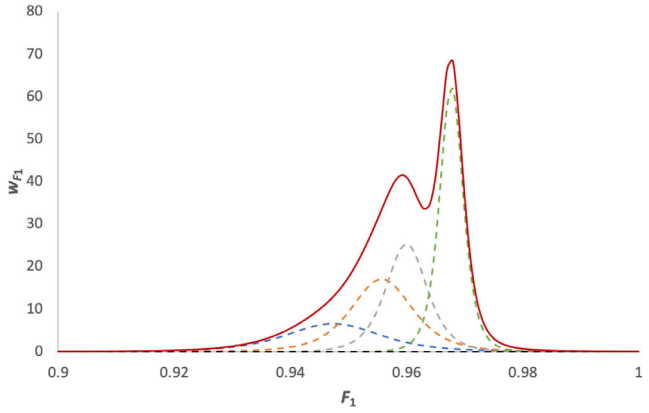

FIGURE 4 The chemical composition distribution (CCD) of an ethylene/1-olefin copolymer may be represented as a superposition of Stockmayer distributions describing the CCD of polymer made on distinct site types.

Analytical methods such as temperature rising elution fractionation (TREF) and crystallization elution fractionation (CEF) can be calibrated with curves that relate elution temperatures to fractions of α-olefin in the copolymer, but these methods don't measure the actual CCD. The peak temperatures of their elution curves depend—often linearly—on the molar fraction of α-olefin in the copolymer; however, the elution curves themselves are not the CCD. For ethylene/α-olefin copolymers, the elution curves depend on the length of the longest ethylene sequences in the chains, which is a function of the copolymer molecular weight, α-olefin molar fraction, and reactivity ratios.[24,25] Other factors, such as crystallization kinetics[26,27] and co-crystallization effects[28,29] muddle even more how elution curves are related to copolymer CCDs.

If this is the case, why has my group published so many articles showing how to deconvolute the CCD of heterogeneous polyolefins into Stockmayer CCD components? Because it works as a shallow solution to a deeper problem, and I believe that a flawed model—if you are aware of its flaws—is better than none. Figure 5

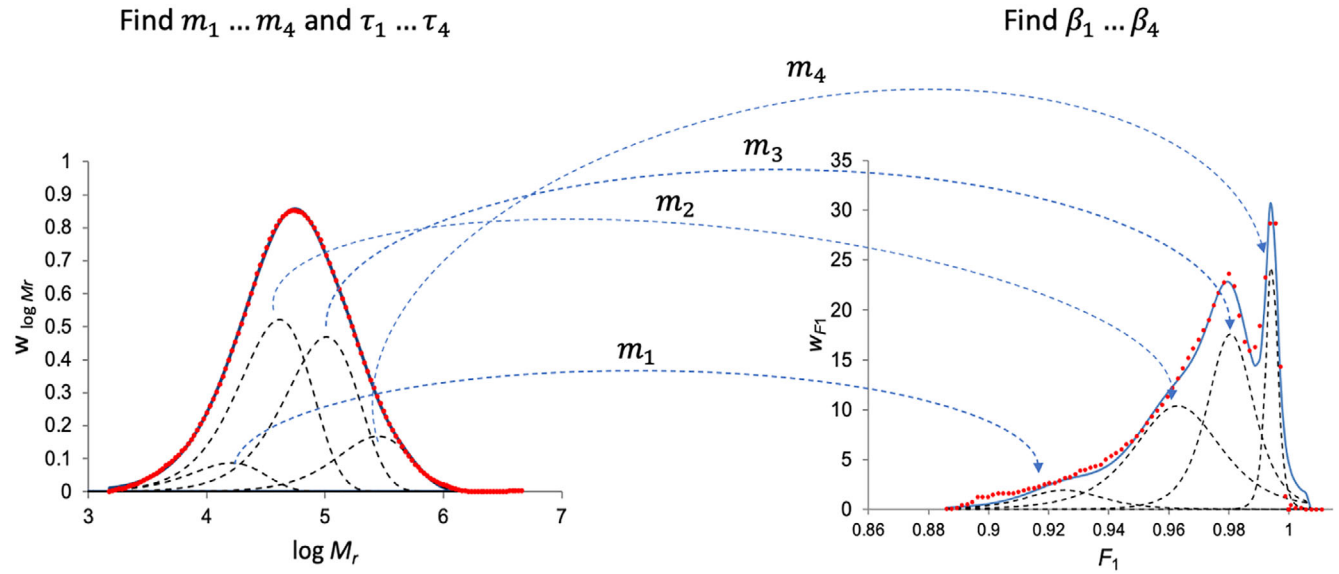

FIGURE 5 Molecular weight distribution (MWD) and chemical composition distribution (CCD) sequential deconvolution: from MWD deconvolution, we find m_i and τ_i and from CCD deconvolution, we find β_i

illustrates how this approach works for an ethylene/α-olefin copolymer made with a Ziegler–Natta catalyst. In the first step, the MWD is deconvoluted into four Flory distributions. This step anchors the next one. We know that GPC can measure the MWD properly, so we can trust these results to estimate τ_1 to τ_4 and m_1 to m_4 (areas under each peak = mass fractions of polymer populations made by each site type). Using the same m_i values, we are free to search only for β_i in the CCD deconvolution step.The model in Figure 5 describes the CCD well. Why did I raise the flag that it might not? Because the values estimated for β_1 to β_4 lack physical meaning. They are nothing more than useful fitting parameters. If we use Equation (5) to calculate the value of the products $(r_1r_2)_1$ to $(r_1r_2)_4$ from β_1 to β_4, we will realize that they are too large. Broad Stockmayer CCDs are needed to fit the experimental profile in Figure 5. From a modelling perspective, the only way to broaden these CCDs is to make β_i too large. (A corollary of this statement is that the copolymer populations identified by CCD deconvolution are unlikely to be made with any coordination catalyst.) The deconvolution algorithm forces the individual CCDs to be broader than reasonable because the model assumes that the TREF or CEF elution profile is formed by the superposition of individual CCDs. But in reality, it is not.

Nobody knows yet how to solve this problem. A theoretically-sound deconvolution model would need to relate how co-crystallization effects, crystallization kinetics, and CEF/TREF column dynamics affect the elution profiles of each polymer population in the heterogeneous copolymer sample. Several models have addressed some of these issues,[30–37] but no model includes all of them. Co-crystallization is especially poorly understood.

Before we leave this topic, let me clarify something: I am not telling you that Equation (4) is a wrong representation of the CCD of olefin copolymers made with single-site-type catalysts. Equation (4) is a direct consequence of the terminal model for copolymerization and, as far as we know, the correct description of the CCD of polyolefins made—instantaneously—with coordination catalysts. The right inference is that TREF and CEF elution curves are functions (still unknown) of Stockmayer CCD components. A similar point could be made for the profiles measured by crystallization analysis fractionation (CRYSTAF), high-temperature thermal gradient interaction chromatography (HT-TGIC), and high-temperature solvent gradient interaction chromatography (HT-SGIC).

Individual MWDs and CCDs unveil a partial, two-dimensional view of the microstructure of olefin copolymers, but to visualize their interrelations, we need to measure their joint MWD × CCD. TREF and GPC can be combined in a cross-fractionation (CFC) instrument that first isolates narrow CCD slices by TREF and then measures their MWDs by GPC. The resulting tridimensional representation of the polyolefin microstructure is often beautiful to behold (Figure 6).

Do we know a fundamental equation that can represent it? Yes. Stockmayer bivariate distribution (we have already discussed its CCD component above) describes

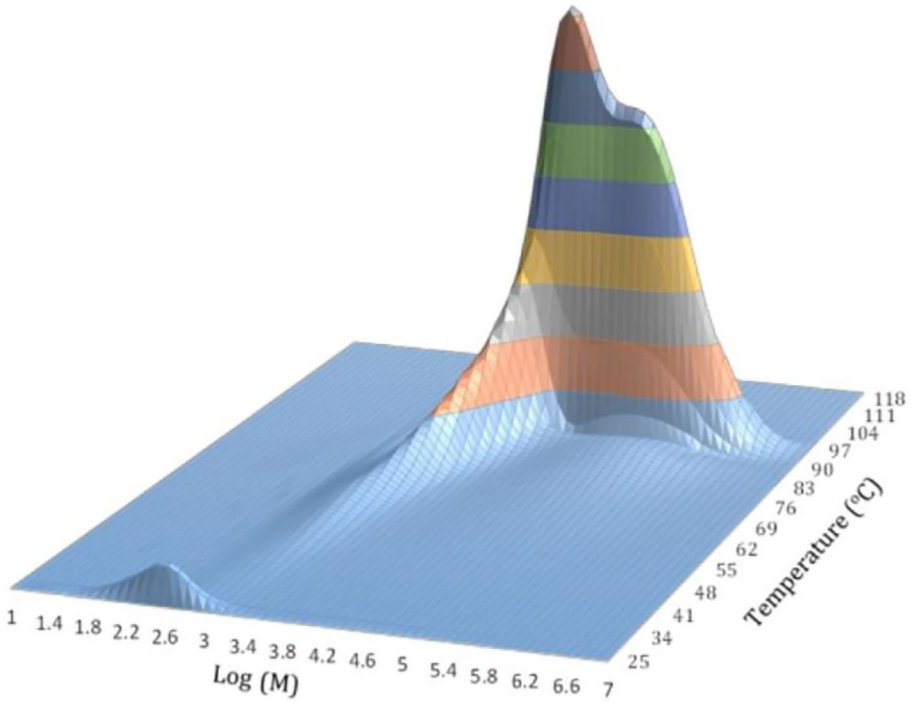

FIGURE 6 Cross fractionation (temperature elution fractionation [TREF] × gel permeation chromatography [GPC]) results of a bimodal ethylene/1-olefin copolymer made with a heterogeneous catalyst

the instantaneous joint MWD × CCD of polyolefins made with a single-site-type catalyst:

$$w_{\log M_r,F_1} = \lambda\left(\frac{M_r}{\overline{M}}\right)^2 \tau^2 \exp\left(-\frac{M_r}{\overline{M}}\tau\right)\sqrt{\frac{M_r/\overline{M}}{2\pi\beta}}\exp\left[-\frac{M_r}{\overline{M}}\frac{(F_1-\overline{F}_1)^2}{2\beta\overline{M}}\right] \quad (6)$$

All variables in Equation (6) were already defined above. Since the distribution has two independent variables, M_r (molecular weight) and F_1 (molar fraction of ethylene), the plot of $w_{\log M_r,F_1}$ is tridimensional (Figure 7).

The simple dome-shaped distributions for single-site-type copolymers assume intricate forms, oftentimes resembling mountain ranges, for polyolefins made with heterogeneous catalysts. Applying the same rules used to describe the MWD and CCD of multiple-site-type polymers, we can represent the MWD × CCD of a polyolefin made with a catalyst having n site types as:

$$W_{\log M_r,F_1} = \sum_{i=1}^{n} m_i w_{\log M_r,F_1,i} \quad (7)$$

Figure 8 simulates the MWD × CCD of a copolymer made with a five-site-type catalyst. Gazing at this profile, I believe you will understand why I was inspired by Tolstoy to say that 'each heterogeneous polyolefin is heterogeneous in its own way.' The combinations of distinct polymer populations are essentially infinite in a polyolefin made with a multiple-site-type catalyst.

Since the MWD can be deconvoluted into several Flory distributions and the CCD into several Stockmayer CCD components—with the caveats I mentioned before—it's reasonable to do the same for the joint MWD × CCD using Stockmayer bivariate distributions. But keep in mind that the limitations that afflict TREF also affect the deconvolution of TREF × GPC cross fractionation. Since we don't know how to account for the crystallization phenomena in the TREF step, we look the other way and pretend they don't exist when we deconvolute the joint MWD × CCD. If you are aware of this shortcoming and don't overstate your findings, you can still get useful models to describe the MWD × CCD of your copolymers.

We still have much to learn here; what is certain is that as a data reduction technique—estimating the values of a few parameters (m_i, τ_i, β_i) that capture the features of a complex bivariate distribution—this method of analysis won't disappoint you.

The distributions discussed above apply only to linear polyolefins. Archie and I also derived equations for polyolefins containing long chain branches (LCB), as extensions of Stockmayer distribution.[38–41] The trivariate MWD × CCD × LCB distribution can, in principle, be used to deconvolute polyolefins with LCBs (formed by terminal branching), but such a study has not been published yet.

2 | LOOKING BACK AT THE LITERATURE

Table 1 lists several papers that use deconvolution methods to investigate the effects of catalyst type and polymerization conditions on polyolefin microstructural distributions and olefin polymerization kinetics. They are classified according to the microstructural distributions they use and whether they also model polymerization kinetics. The table footnote defines each of the distributions and the analytical methods used to measure them.

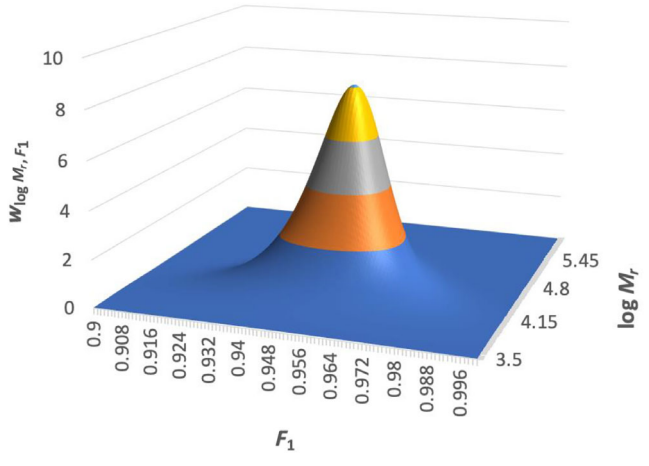

FIGURE 7 Stockmayer bivariate distribution for an ethylene/1-olefin copolymer made with a single-site catalyst. Model parameters: $\overline{F}_1 = 0.9526$, $\beta = 0.0452$, $\tau = 4.23 \times 10^{-3}$

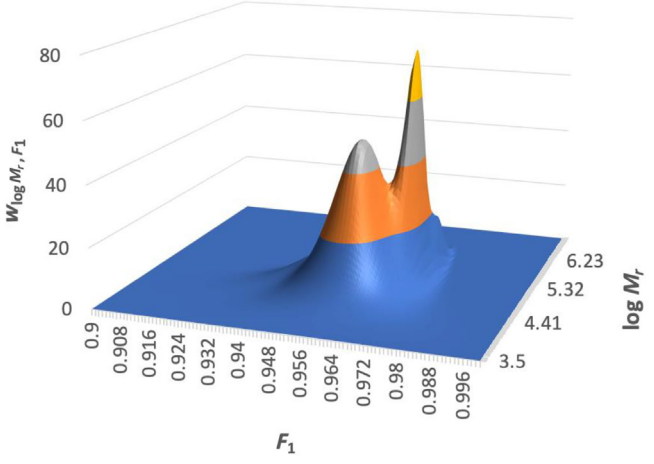

FIGURE 8 Representation of the molecular weight distribution (MWD) × chemical composition distribution (CCD) of an ethylene/1-olefin copolymer made with a five-site-type catalyst as a superposition of five Stockmayer bivariate distributions

TABLE 1 Articles on polyolefin deconvolution methods

No.	References	MWD	CCD	MWD × CCD	SCB	CSLD	Kinetics
1	[20,23,42–115]	X					
2	[22,116–126]	X	X				
3	[127–130]			X			
4	[131–139]	X			X		
5	[140–143]	X				X	
6	[42,144–153]	X					X

Note: MWD: molecular weight distribution (GPC)/CCD: chemical composition distribution (TREF, CEF, CRYSTAF, HT-TGIC, HT-SGIC)/SCB: short chain branch distribution across the MWD (GPC-IR)/ MWD × CCD: bivariate molecular weight and chemical composition distribution (CFC)/CSLD: comonomer sequence length distribution (13C NMR)/Kinetics: multiple-site-type polymerization kinetics.
Abbreviations: CEF, crystallization elution fractionation; CRYSTAF, crystallization analysis fractionation; GPC, gel permeation chromatography; HT-SGIC, high-temperature solvent gradient interaction chromatography; HT-TGIC, high-temperature thermal gradient interaction chromatography; TREF, temperature rising elution fractionation.

Two seminal papers on MWD deconvolution were published in 1993, one by Vickroy et al.[20]—which I already mentioned above—and another by Kissin.[42] The paper by Vickroy and coworkers proposed a simple procedure to deconvolute a broad MWD into several Flory components using a commercial software, as an user-friendly alternative to the method proposed by Broyer and Abbott in 1982.[43] Kissin's paper had a more ambitious scope: in addition to proposing a MWD deconvolution method, he also showed how to use the information obtained through MWD deconvolution to estimate polymerization kinetic constants for each catalyst site type. The authors of both papers were industrial researchers, indicating the commercial importance of this modelling approach in the early 90s. A couple of years later, Kissin wrote another remarkable paper in which he extended the MWD deconvolution method to polyethylene, ethylene/α-olefin copolymers, polypropylene (isotactic and syndiotactic), and free-radical polystyrene. He also suggested a method to correct for GPC peak broadening.[44]

Most—but not all—MWD deconvolution methods cited in the first row of Table 1 used Flory distribution to describe the MWD of polyolefin populations made on each site type. Some authors reasoned that the kinetic constants of active sites of the same type didn't have a single value but instead were distributions of values that arose when the catalyst sites interacted with the heterogeneous catalyst support.[45–50] Remembering the definition of τ in Equation (2), this means that the values of τ should follow a distribution given as the ratio of the distributions for the propagation and chain transfer frequencies

$$\Phi(\tau) = \frac{\sum \Theta\left(f_{t_i}\right)}{\Xi\left(f_p\right)} \tag{8}$$

where $\Phi(\tau)$, $\Theta\left(f_{t_i}\right)$, and $\Xi\left(f_p\right)$ are the distributions for τ, f_{t_i}, and f_p, respectively.

It is reasonable to assume that sites of the same type may have different kinetic constants due to their interactions with a non-uniform catalyst surface. The main problem is that we don't know what these distributions are and we can't measure them. The solution to this conundrum has been to make educated guesses, such as the log-normal distribution,[48,49] the Wesslau equation,[45–47] and sometimes unspecified peak functions.[50] Fewer site types are needed to fit the MWD with these broader distributions, but the risk of finding multiple solutions also increases. In 1998, I proposed a related (and somewhat awkward) method that still used Flory distribution but with a broadening function associated with the parameter τ.[49] I will discuss the original and a modified version of this method in the next section of this article.

Because it is easier to use, deconvoluting the MWD into discrete Flory components has become the standard method in academic and industrial studies. This approach has been used to understand the distribution of active site types in Ziegler–Natta catalysts for propylene polymerization as a function of polymerization temperature and time, type of cocatalyst and electron donor, copolymerizations with other α-olefins, and catalyst synthesis conditions.[51–66] Similar deconvolution studies were used to understand the effect of polymerization conditions and catalyst formulations for the polymerization of ethylene and α-olefins with Ziegler–Natta[67–81] and Phillips/chromium catalysts.[82–84] Other studies used MWD deconvolution to identify active site populations for the polymerization of 1-octene,[85] 1-hexene,[86–89] and 1-butene[90,91] with Ziegler–Natta catalysts. An alternative MWD deconvolution algorithm, using the cumulative version of Flory distribution, has also been proposed but has not been widely adopted.[92–94]

MWD deconvolution methods have also been used to understand the behaviour of metallocenes and post-metallocenes—homogeneous or heterogenized—either because they deviated from their expected single-site-type behaviour or because two or more single-site-type catalysts were combined to design a multiple-site-type catalyst.[95–107]

As a result of the widespread use of the Flory-MWD deconvolution approach, this method has been implemented in Polymer Plus and Aspen Dynamics to simulate steady-state and dynamic olefin polymerization processes.[108–110] All other process simulators that assume the presence of several site types that make polyolefins using the classic coordination polymerization mechanism implicitly or explicitly incorporate this concept in their codes.

This method has also been used in some applications that deviate from its original intent, such as to propose analytical solutions for the visbreaking of polypropylene.[111] In a recent novel application of the MWD deconvolution method, Pernusch et al. quantified how poisons originating from chemically recycled plastic waste affected the performance of Ziegler–Natta catalysts.[112] Fortuny et al.[113] proposed a dynamic version of Flory distribution to account for the change in polymerization conditions in batch and semi-batch laboratory reactors; they concluded that fewer sites were needed under these conditions because part of the broadening was related to non-steady state polymerization conditions, as illustrated in Figure 2.

Less attention has been paid to the non-linear optimization method used to fit experimental MWDs with Flory distributions—the solution of Equation (3). With few exceptions, no details are mentioned in the articles. Hamielec and I[23] compared the Levenberg–Marquardt and the Golub–Pereyra methods. (The latter is designed to deal with estimation problems that combine linear, m_i, and non-linear, τ_i, parameters.) Singh et al.[114] proposed a real-coded genetic algorithm to deconvolute MWDs, attempting to move from local minima to the global minimum. Recently, Patil et al.[115] proposed a numerical method—jitter differential evolution—to deconvolute MWDs that they claim offers some advantages over the previous deconvolution algorithms.

MWD deconvolution into multiple Flory distributions is now an established method for polyolefins, largely because it is simple to use and converges to unique solutions. Unfortunately, these advantages come with some pitfalls. If you let me use another photographic analogy, we may envision deconvolution as a lens through which we peer into the causes of broad MWDs. Lenses highlight certain aspects of a scene but distort others. We must keep this in mind when we look for explanations based on MWD deconvolution results. First, these methods can identify only the minimum number of active site types present in a catalyst: many more site types—making MWDs that overlap too much to be identified when minimizing Equation (3)—may exist in the catalyst. On the other hand, several other phenomena may trick the deconvolution method into identifying spurious active sites, such as support effects,[45–50] intraparticle mass and heat transfer gradients,[154] reactor residence time distribution effects,[155–157] and GPC peak broadening.[42] Examples of the bad and the ugly applications of MWD deconvolution methods often appear when they are used without proper consideration of these confounding factors.

The second row of Table 1 lists articles that went one step beyond and deconvoluted the CCD of polyolefins in addition to their MWDs (MWD + CCD). In 1995, Hamielec and I proposed a model to represent the ideal TREF profile of ethylene/α-olefin copolymers as a superposition of the CCD components of Stockmayer distribution.[22] We used the term ideal fractionation 'to indicate that we expect the separation mechanism to be controlled only by copolymer composition or stereoregularity, free of cocrystallization effects, molecular weight influences, and peak broadening due to axial dispersion and crystallization kinetics'. Now, we know that these conditions are never obeyed, but this method is still useful to represent broad CCDs as the sum of narrow, symmetric, and theoretically sound distributions. I explained some of these fine points in more detail in a previous review on the use of polyolefin microstructural models.[116]

Based on a similar rationale, but using a slightly different approach, da Silva Filho et al.[117] used Flory distribution to deconvolute the MWD and normal distributions to deconvolute TREF and CRYSTAF profiles of ethylene/1-butene copolymers made with an industrial Ziegler–Natta catalyst. They first deconvoluted the MWD to estimate the parameters τ_i and m_i; keeping the same values for m_i, they estimated the TREF elution temperatures, T_{e_i}, or CRYSTAF crystallization temperatures, T_{c_i}, and their respective standard deviations, σ_i. Kissin and Fruitwala also used normal distributions to fit CRYSTAF profiles of ethylene/1-hexene copolymers and isotactic polypropylene.[118]

Veering through a different path, Kissin et al.[119] used Lorenz distributions to deconvolute TREF profiles of ethylene/1-butene copolymers. Even though they also deconvoluted the MWDs using Flory distributions, they didn't follow the sequential approach of de Silva Filho et al.[117]; instead, they did the two deconvolutions independently, finding that fewer site types were needed to describe the MWD than the TREF profile. They justified this discrepancy by proposing that some site types had different reactivity ratios but made polymers with similar

MWDs, which overlapped too much to be separated by MWD deconvolution.

Wang et al.[120] also used Flory and Lorenz distributions to deconvolute the MWD and TREF profiles of polypropylene made with a Ziegler–Natta catalyst in a stopped-flow reactor. Even though these distributions fitted the data, it is important to realize that under the very short residence times (typically below 1 s) of stopped flow reactors, Flory distribution may not be fully established, rendering this approach meaningless.[121,122]

The deconvolution of TREF, CEF, and CRYSTAF profiles of LLDPE samples that have soluble fractions present an additional challenge. The so-called soluble peak is made of polymer chains with high α-olefin fraction that don't crystallize during the analysis; therefore, they cannot be deconvoluted into Stockmayer CCD components using the method Archie and I described in our 1995's paper.[22] One of my PhD students proposed a method to handle these samples by combining MWD deconvolution with Flory distributions and TREF deconvolution with the cumulative version of the Stockmayer CCD component.[123,124]

Using MWDs and CCDs simulated as superpositions of several Stockmayer distributions—which I am calling digital MWDs and CCDs in this article—Anantawaraskul et al.[125] proposed a simultaneous deconvolution method to retrieve the model parameters used to generate the multiple-site-type distributions. Finding initial guesses for these non-linear optimization problems can be challenging: to overcome this hurdle, Nanthapoolsub et al.[126] used a genetic algorithm to estimate the parameters for the simultaneous deconvolution of the MWD and CCD of polyolefins.

The arrival of commercial TREF × GPC cross fractionation instruments popularized their use in industrial and academic laboratories.[158] The next logical step in microstructural modelling techniques was to deconvolute the joint MWD × CCD that can be so beautifully measured by CFC (third row, Table 1). Anantawaraskul et al.[127] compared four different deconvolution strategies using digital ethylene/1-olefin copolymer microstructures simulated with a five site-type catalyst: (1) MWD–short chain branch (SCB) (see the next paragraph for more details), (2) simultaneous MWD and CCD, (3) simultaneous MWD–SCB and CCD, and (4) joint MWD × CCD. They found that deconvolution of the joint MWD × CCD generated the most accurate estimates of the parameters used to create the digital microstructures, but these models didn't include non-ideal effects such as peak broadening and co-crystallization effects. Hornchaiya et al.[128] tested the joint MWD × CCD deconvolution method using experimental CFC profiles of blends of two or three ethylene/1-butene copolymers made with a metallocene. The values estimated from deconvolution (M_n, 1-butene molar fraction, and mass fractions of each blend component) matched—with a few exceptions—those measured for the blend components, even though the method didn't account for the noticeable co-crystallization of some blend components. They also applied their method to deconvolute the CFC of ethylene/1-butene copolymers made with a Ziegler–Natta catalyst into multiple Stockmayer distributions. Chayrattanoroj and Anantawaraskul[129] extended this joint deconvolution approach for digital multiple-site-type copolymers made in dual reactors in series (bimodal polyethylenes). Finally, Khayanying and Anantawaraskul[130] used a genetic algorithm to improve the convergence properties of their joint MWD × CCD deconvolution method.

The fourth row of Table 1 lists references for the deconvolution of MWD–SCB profiles measured by GPC-IR. The MWD–SCB is measured by coupling an infrared detector to the GPC unit. The infrared (IR) detector quantifies the average SCB frequency, or 1-olefin fraction, as a function of polymer molecular weight. Tso and DesLauriers compared the level of microstructure details this method provides in relation to TREF separation.[159] Dick Abbot, from Paxon, and I—in collaboration with colleagues from Lab Connections—proposed the first method to deconvolute the MWD–SCB of ethylene/α-olefin copolymers in 1996.[131] At the time, the use of on-line IR detectors with high-temperature GPC was rare, but Lab Connections sold a sample collection unit (LC-Transform) that could be used to deposit the polymer fractions exiting the GPC column on a germanium disk. After GPC fractionation, the disk could be connected to a Fourier-transform IR spectrometer to measure the SCB distribution as a function of the polymer's molecular weight. Today, this analysis is done much more easily with commercial online high-temperature IR detectors.[132]

Figure 9 illustrates how this method works—the mathematical details can be found in our original publication[131] or in Soares and McKenna.[133] The main hypotheses behind this method are easy to grasp:

1. The MWD of a polyolefin made with a multiple-site-type catalyst can be represented as a superposition of several Flory distributions.
2. The average α-olefin fraction (or SCB frequency) of an ethylene/α-olefin copolymer made with a single-site-type catalyst doesn't depend on its molecular weight.[133]
3. The SCB frequency measured across the MWD of an ethylene/α-olefin copolymer made with a multiple-site-catalyst is the weighted average of the SCB frequencies of the ethylene/α-olefin copolymer populations made on each site type.

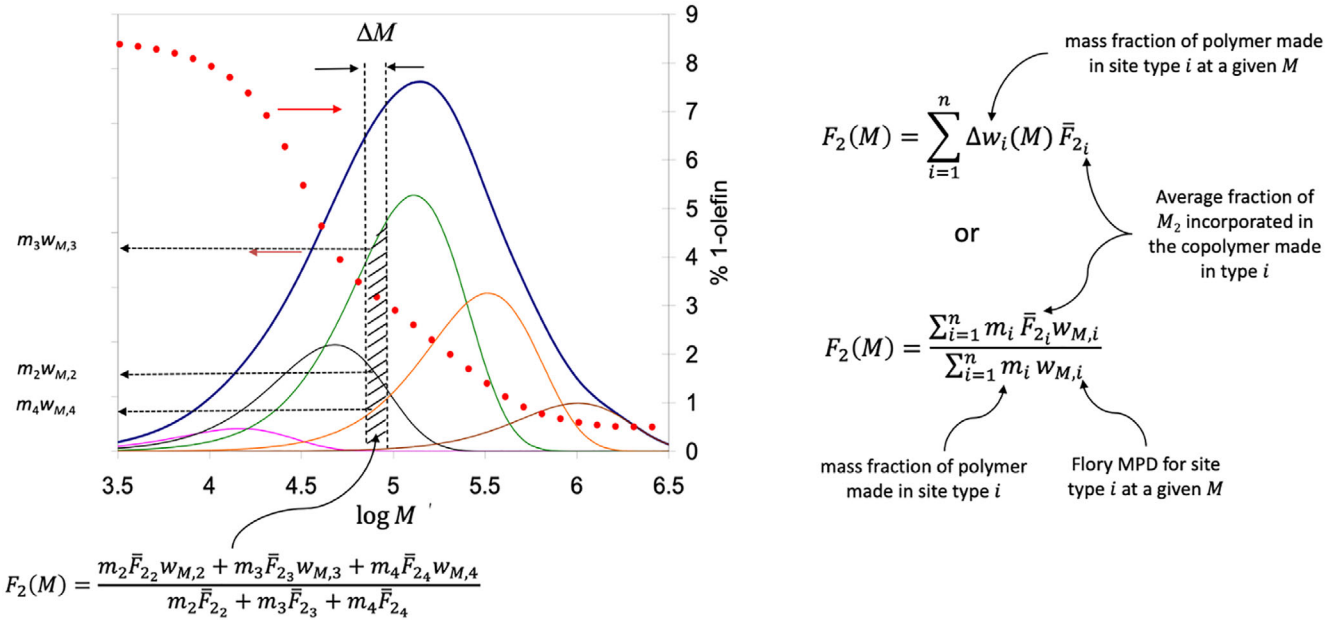

FIGURE 9 Molecular weight distribution (MWD)–short chain branch (SCB) (measured by gel permeation chromatography-infrared [GPC-IR]) deconvolution. MDP, most probable distribution.

4. The fraction of α-olefin copolymerized by each site type can be found by fitting the experimental GPC-IR plot, shown in Figure 9, as a superposition of the MWD–SCB for each site type.

If we apply this procedure to copolymers made over a wide range of ethylene/α-olefin ratios, we can also estimate the comonomer reactivity ratios per site type using the Mayo–Lewis equation.[131] Faldi and Soares further explored the benefits and limitations of this approach.[134]

In a more elaborate study, Chen et al.[135] used the MWD–SCB deconvolution method to quantify how the composition of ethylene/1-hexene copolymers made on each site type of a Ziegler–Natta catalyst depended on polymerization time and 1-hexene concentration in the reactor. They concluded with a statement revealing the limitations of this method 'What this method cannot do is elucidate the chemical nature of the identified active site types, nor determine if more site types may be present in the catalyst. The model is restricted to the determination of the *minimum* number of active site types needed to describe a given polyolefin microstructure based on the mechanism accepted for coordination polymerization. We can be sure that fewer site types could not describe the microstructure of the polymers under study, but we must remain silent regarding the presence of additional site types that may make polymers with microstructures that partially overlap with those microstructures in the model identified. For most engineering applications, however, Occam's razor is a good principle to go by, and the minimum number of active sites should suffice.'[135]

This method has also been applied to industrial and pilot plant reactors. In 2007, Francisco Pérez Valencia and I developed a proprietary steady-state process model to predict the MWD–SCB of HDPE resins made in a series of reactors for Repsol.[136] Tian et al.[137] combined the MWD–SCB deconvolution approach with structure–property relationships to simulate the performance of bimodal polyethylene resins made in the Borstar process. Feng et al.[138] found out that the simultaneous deconvolution of the MWD–SCB of ethylene/1-hexene copolymers made in a continuous gas-phase pilot plant reactor worked better than the sequential method used in previous publications. Recently, Göpperl et al.[139] have also used this method to interpret the effect of the titanation temperature on the evenness of the MWD–SCB of Ziegler–Natta catalysts.

In many ways, MWD–SCB deconvolution is an excellent compromise. It is not as detailed as the MWD + CCD or MWD × CCD deconvolutions, but it is not subject to some of the questionable simplifications the latter methods must make. Its main limitation is the low signal-to-noise ratio for samples with low SCB frequencies, especially at the tails of the MWD; luckily, the development of more sensitive on-line detectors is making this a lesser concern.

None of the methods discussed up to now can describe the comonomer sequence length distribution

(CSLD) of olefin copolymers. The CSLD is often expressed in terms of dyad, triad, tetrads, and higher *n*-ads for ethylene and α-olefins. For these predictions, we need to include ^{13}C NMR data in our analysis. Cheng[160–164] published a series of captivating papers—the ones I cited are part of a longer list—between the late 80s and early 90s. In them, he estimated the reactivity ratios, r_{1_i} and r_{2_i}, for each catayst site type by quantifying the CSLD of ethylene/α-olefin copolymers made with multiple-site-type catalysts using statistical models, such as Bernoullian, terminal, and penultimate models. Even though these articles unravelled fine details about the copolymer microstructure, they suffered from a few drawbacks.[140] Their main limitation was to estimate the mass fractions of polymer populations made on each site type using only ^{13}C NMR data. Since ^{13}C NMR measures the average intensity of the *n*-ads for all polymer populations in the sample, multiple solutions are unavoidable.

We proposed a solution to this shortcoming in a series of three papers using a method we called the integrated deconvolution estimation model—IDEM (Table 1, fifth row).[140–142] IDEM first deconvolutes the MWD into several Flory distributions to estimate the number of site types and the mass fraction of polymer made on each of them, like any other MWD deconvolution method. Then, IDEM uses these mass fractions with triad or tetrad data to fit the CSLD of the whole polymer and estimate the reactivity ratios of each site type. Using the mass fractions of each polymer population adds a constraint that makes it easier to find unique solutions for this non-linear estimation problem.

We used only digital microstructures in the first article in the series to validate our method and found that using tetrads led to better reactivity ratio estimates.[140] We also showed that the estimates could be improved if we removed the comonomer sequences with near-linear dependency. In our second paper, we applied IDEM to two series (made with and without H_2) of copolymers synthesized with a commercial $TiCl_4/MgCl_2$ Ziegler–Natta catalyst under different ethylene/1-butene ratios.[142] IDEM could estimate the reactivity ratio per site type for ethylene, r_{1_i}, more accurately than for 1-butene, r_{2_i}, because it is difficult to produce ethylene/1-butene copolymers with a high 1-butene content using Ziegler–Natta catalysts. (This limitation is not exclusive of IDEM; it afflicts any other estimation method for ethylene/α-olefins reactivity ratios with Ziegler–Natta catalysts.) Finally, in the third publication, we investigated the effect of analyzing the samples by ^{13}C NMR in different laboratories, ours and Dow Chemical's.[142] Even though the two laboratories followed different analytical protocols, the reactivity ratio estimates agreed reasonably well. Cheng et al.[143] also used a similar method to model the CSLD of ethylene/propylene copolymers made with a vanadium-based catalyst.

MWD deconvolutions have also been used to estimate the polymerization kinetic constants of the different site types in multiple-site-type catalysts. In 1993, Kissin published his landmark paper on ethylene homopolymerization kinetics with a Ziegler–Natta catalyst.[42] He later extended this method to several other olefin polymerization systems and suggested new polymerization mechanisms, such as β-agostic stabilization, to explain the effects of α-olefin and H_2 on ethylene polymerization kinetics with Ziegler–Natta catalysts.[144–147] Many of the subsequent articles written by other authors that estimated polymerization kinetic parameters benefited from Kissin's teachings.[148–150] Recently, Charoenpanich et al.[151] devised a new approach better suited to model the MWD and polymerization kinetics of bulk propylene polymerization made in two reactors in series using limited industrial product development data.

You may wonder how MWD deconvolution can be used to estimate polymerization kinetic constants. If you use Equation (3) to deconvolute a MWD, the only information you will get is n, τ_i, and m_i, none of which are linked to time-dependent polymerization kinetic curves. Indeed, some of the ugly applications of this method come about when one doesn't realize that one can only estimate polymerization kinetic parameters if one has access to reliable time-dependent monomer consumption rates and/or polymer production data.

The trick is to add time to the deconvolution recipe by deconvoluting MWDs made at different polymerization times. I will explain how the process works without going into nitty-gritty mathematical details. In its simplest form, the polymerization rate, R_{p_i}, of a given site type depends on the polymerization temperature, T; the concentrations of ethylene, propylene, and α-olefins at the active sites, $[M]_j$; the site activation and deactivation rate constants, k_{a_i} and k_{d_i}; and the propagation rate constant, k_{p_i}

$$R_{p_i} = f\left(k_{a_i}, k_{p_i}, k_{d_i}, [M]_j, T\right) \tag{9}$$

The particular form of the function $f\left(k_{a_i}, k_{p_i}, k_{d_i}, [M]_j, T\right)$ depends on the polymerization mechanism that fits your experimental data,[133] but we don't need to worry about specific details to understand how the method works.

When we integrate Equation (9), we get the polymer yield per site type after a certain polymerization time, t

$$Y_{p_i}(t) = \overline{M}_i \int_0^t R_{p_i} \mathrm{d}t = \overline{M}_i \int_0^t f\left(k_{a_i}, k_{p_i}, k_{d_i}, [M]_j, T\right) \mathrm{d}t \tag{10}$$

here $\overline{M}_i$ is the average molar mass of the repeating unit of the polymer population made on site type i.

The yield of a multiple-site-type catalyst—which we can measure by gravimetry or by integrating the rate of monomer consumption as a function of time—is the sum of all the yields per site type

$$Y_p(t) = \sum_{i=1}^{n} Y_{p_i} = \sum_{i=1}^{n} \overline{M}_i \int_0^t R_{p_i} \mathrm{d}t = \sum_{i=1}^{n} \overline{M}_i \int_0^t f\left(k_{a_i}, k_{p_i}, k_{d_i}, [M]_j, T\right) \mathrm{d}t \quad (11)$$

The parameter m_i in Equation (3) is related to these polymer yields through the equation

$$m_i(t) = \frac{Y_{p_i}(t)}{Y_p(t)} = \frac{\overline{M}_i \int_0^t f\left(k_{a_i}, k_{p_i}, k_{d_i}, [M]_j, T\right) \mathrm{d}t}{Y_p(t)} \quad (12)$$

If you deconvolute the MWD of a polyolefin made at the same $[M]_j$ and T but different polymerization times, you will find a set $m_i(t)$ values. You can then fit this data with Equation (12) to estimate k_{a_i}, k_{d_i}, and k_{p_i} for each site type in the catalyst. Whether we need to know the polymerization kinetic parameters for each site type is debatable[10,133]—from a pragmatical point of view, often the kinetics of multiple-site-type catalysts can be described with a single set of lumped constants[152,153]—but Equation (12) teaches how to estimate them.

Figure 10 shows the timeline for the development of the polyolefin deconvolution methods reviewed in this section.

Several of these methods are used in conjunction with deconvolution software, such as BorMol,[165] to provide data for product development and polymerization process simulators. They are powerful lenses that help us inspect the convoluted phenomena happening when olefins are polymerized with any multiple-site-type catalyst. Therein lies their enduring appeal.

3 | TAKING A DIFFERENT LOOK AT DECONVOLUTION

As discussed above, the deconvolution of MWD into several Flory distributions has become the standard method to interpret the effect of different conditions on the microstructure of polyolefins made with multiple-site-type catalysts. Most of these models assumed the existence of a discrete number of active site types. Even though the classic deconvolution method works well and generates useful models that can describe and predict the MWD of polyolefins, it has always bothered me a little that typically four to five site types are needed to describe the MWD of Ziegler–Natta polyolefins—and even more for polyolefins made with Phillips catalysts. How would these sites differ? As mentioned in the previous section, other models have addressed this concern before.[45–50] Below, I will propose a reformulation of these alternative methods—a new lens—to look at this problem in the form of a speculative, but I hope useful, thought experiment.

Several years ago, I proposed an alternative mechanism to explain broad MWDs using fewer site types.[49] This paper has attracted little attention, and justly so, but I

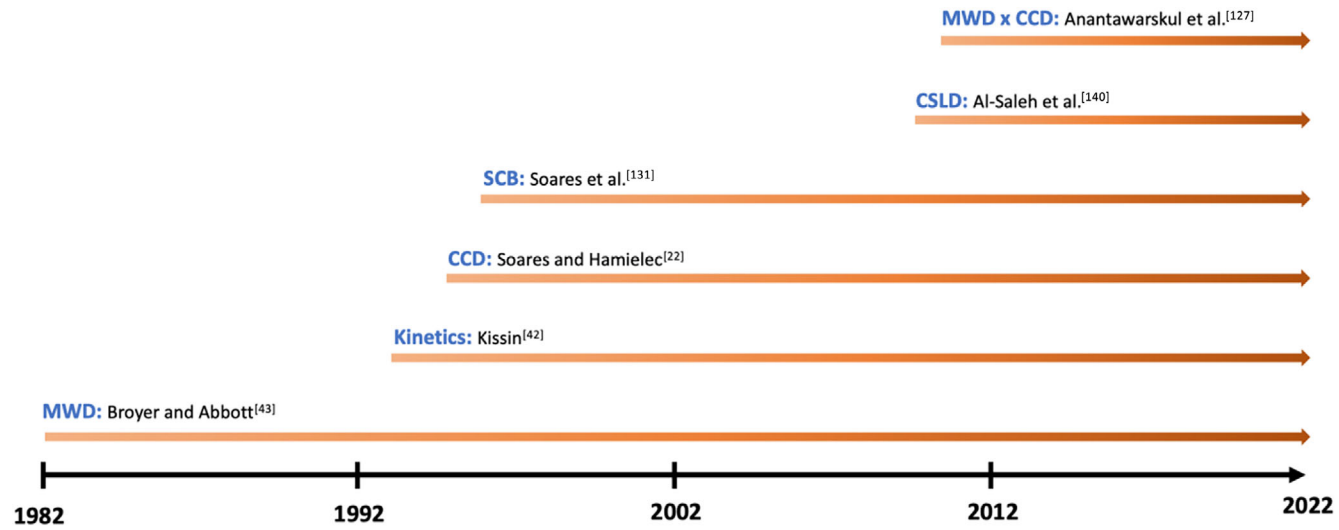

FIGURE 10 Timeline for articles on polyolefin microstructure deconvolution. CCD, chemical composition distribution. CSLD, comonomer sequence length distribution. MWD, molecular weight distribution. SCB, short chain branch

still think it contained a valid core idea: Instead of assuming that n site types with n distinct τ values are needed to model the MWD of polyolefins, why not assume that these MWDs could be modelled with one or two site types with different τ distributions? This is a reasonable supposition when we allow for the heterogeneity of the catalyst support. Even metallocene catalysts make polymers with broader MWDs when supported on inorganic carriers.[106,107]

Let's simplify the definition of τ in Equation (2) by considering that transfer to H_2 is the dominant chain transfer mechanism

$$\tau = \frac{f_{t_H}}{f_p} \tag{13}$$

Most of the models discussed in the previous section assumed that the transfer and propagation frequencies for sites of the same type had the same value. Instead, if we assume that these frequencies are described by normal distributions, we can write

$$N\left(f_p\right) = \frac{1}{\sigma_{f_p}\sqrt{2\pi}} \exp\left[-\frac{1}{2}\left(\frac{f_p - \mu_{f_p}}{\sigma_{f_p}}\right)^2\right] \tag{14}$$

$$N\left(f_{t_H}\right) = \frac{1}{\sigma_{f_{tH}}\sqrt{2\pi}} \exp\left[-\frac{1}{2}\left(\frac{f_{t_H} - \mu_{f_{tH}}}{\sigma_{f_{tH}}}\right)^2\right] \tag{15}$$

Following this reasoning, we can define the distribution of values for the parameter τ as a ratio of two normal distributions

$$F_Z(\tau) = \frac{N\left(f_{t_H}\right)}{N\left(f_p\right)} \tag{16}$$

The ratio distribution of two uncorrelated normal distributions is expressed as[166]

$$F_Z(\tau) = \frac{1+\mu\tau\sigma^2}{\sqrt{2\pi}\frac{\delta_p}{\sigma}\left(1+\tau^2\sigma^2\right)^{2/3}} \exp\left[-\frac{\sigma^2(\tau-\mu)^2}{2{\delta_p}^2\left(1+\tau^2\sigma^2\right)}\right] \operatorname{erf}\left(\frac{1+\mu\tau\sigma^2}{\delta_p\sqrt{2+2\tau^2\sigma^2}}\right) \tag{17}$$

where $\mu = \mu_{f_{tH}}/\mu_{f_p}$, $\sigma = \sigma_{f_p}/\sigma_{f_{tH}}$, and $\delta_p = \sigma_{f_p}/\mu_{f_p}$.

For the range of values of practical interest, the error function in Equation (17) tends to one, and Equation (17) becomes

$$F_Z(\tau) = \frac{1+\mu\tau\sigma^2}{\sqrt{2\pi}\frac{\delta_p}{\sigma}\left(1+\tau^2\sigma^2\right)^{2/3}} \exp\left[-\frac{\sigma^2(\tau-\mu)^2}{2{\delta_p}^2\left(1+\tau^2\sigma^2\right)}\right] \tag{18}$$

Figure 11 shows the distribution for τ calculated with Equation (18). The values for the distribution parameters in Figure 11 are arbitrary; I used large standard deviations to quantify the effect of surface heterogeneity on f_p and f_{t_H}, but not so large as to generate meaningless

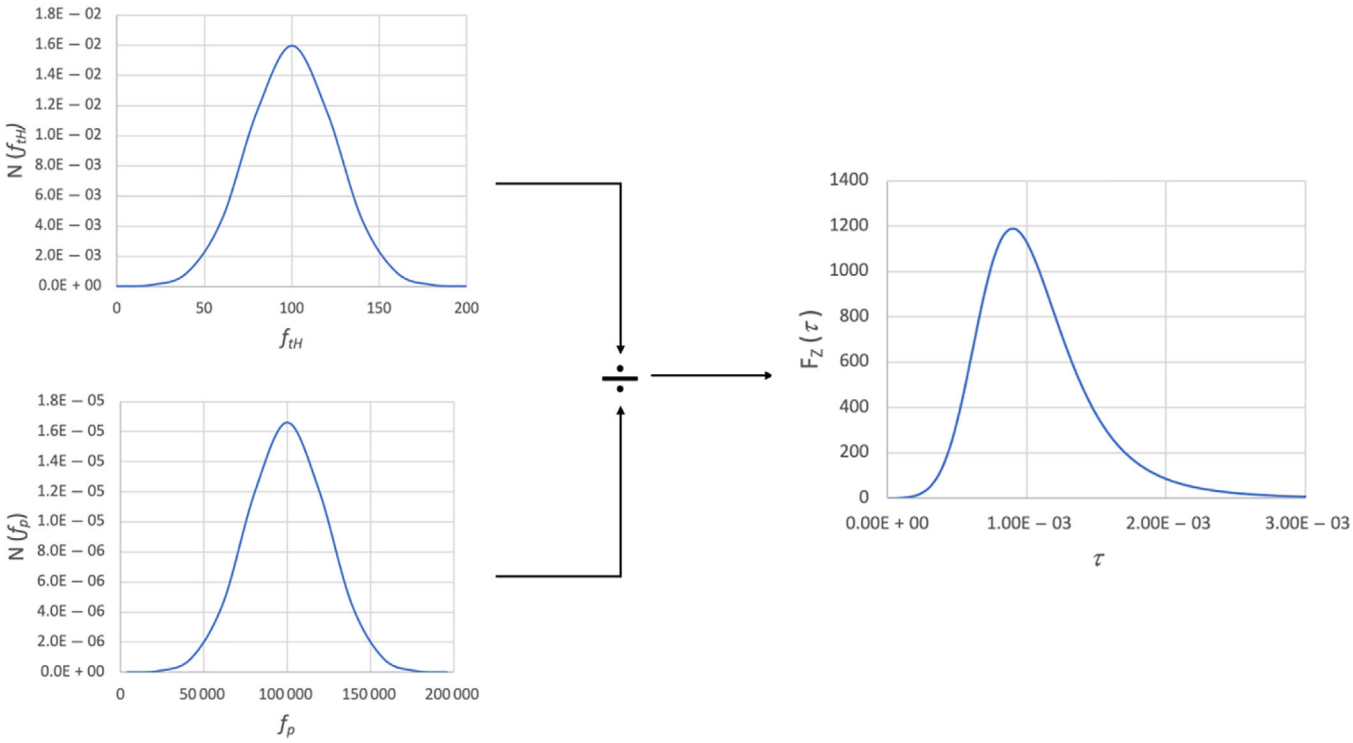

FIGURE 11 Ratio distribution for τ when the propagation and chain transfer frequencies follow normal distributions. Distribution parameters: $\mu_{f_p} = 1 \times 10^5$, $\sigma_{f_p} = 2.4 \times 10^4$, $\mu_{f_{tH}} = 100$, $\sigma_{f_{tH}} = 25$

negative frequencies.Equation (18) helps us visualize how τ varies if we assume that f_p and f_{t_H} are normally distributed. Unfortunately, the ratio distribution cannot be used to calculate MWDs because the mass of polymer produced by an active site is proportional to its propagation frequency, f_p, and each $\tau = f_{t_H}/f_p$ ratio in the x-axis may result from infinite combinations of f_p and f_{t_H}. To calculate the MWD, we need to use the less convenient expression,

$$w_{\log M_r} = \lambda \left(\frac{M_r}{\overline{M}}\right)^2 \frac{\int_0^\infty f_p N(f_p) \left[\int_0^\infty N(f_{t_H}) \left(\frac{f_{t_H}}{f_p}\right)^2 \exp\left(-\frac{M_r}{\overline{M}} \frac{f_{t_H}}{f_p}\right) \mathrm{d}f_{t_H}\right] \mathrm{d}f_p}{\int_0^\infty f_p N(f_p) \mathrm{d}f_p} \tag{19}$$

(Note that $\int_0^\infty f_p N(f_p) \mathrm{d}f_p = \mu_{f_p}$.)

Figure 12 compares the broader MWD calculated with Equation (19) with Flory distribution using the average values for f_p and f_{t_H}.Even though f_p and f_{t_H} follow broad normal distributions, the effect on the MWD is relatively modest, with the dispersity increasing from 2.0 to only 2.2. If we deconvolute the distribution calculated with Equation (19) in Figure 12, we will find that two Flory distributions describe the results well (Figure 13).

This is an interesting result: if the propagation and chain transfer frequencies of a single-site-type catalyst are affected by the support, then the classic MWD deconvolution procedure would mistakenly attribute the broadening to the presence of a second site type.

These results also show that the ratio distribution can describe moderate MWD broadening—like the

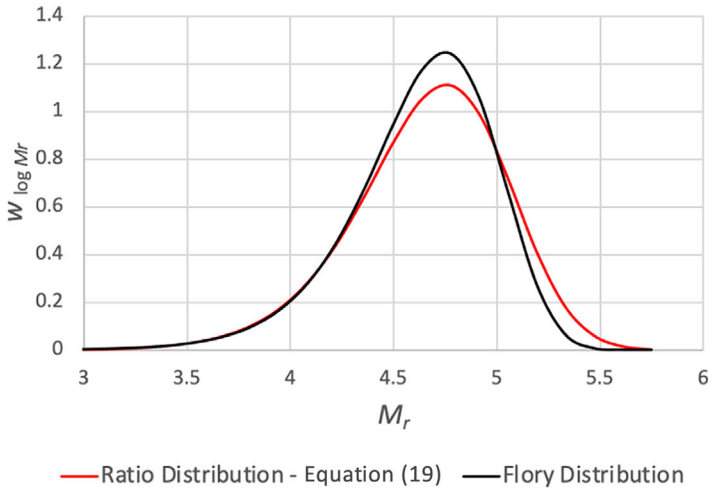

Distribution	M_n	M_w	M_w/M_n
Flory	28 000	56 000	2.0
Equation (19)	29 000	65 000	2.2

FIGURE 12 Molecular weight distribution (MWD) calculated with Equation (19) in comparison with the equivalent Flory distribution. Frequency distribution parameters: $\mu_{f_p} = 1 \times 10^5$, $\sigma_{f_p} = 2.5 \times 10^4$, $\mu_{f_{tH}} = 100$, $\sigma_{f_{tH}} = 25$. For Flory distribution, $\sigma_{f_p} = \sigma_{f_{tH}} = 0$

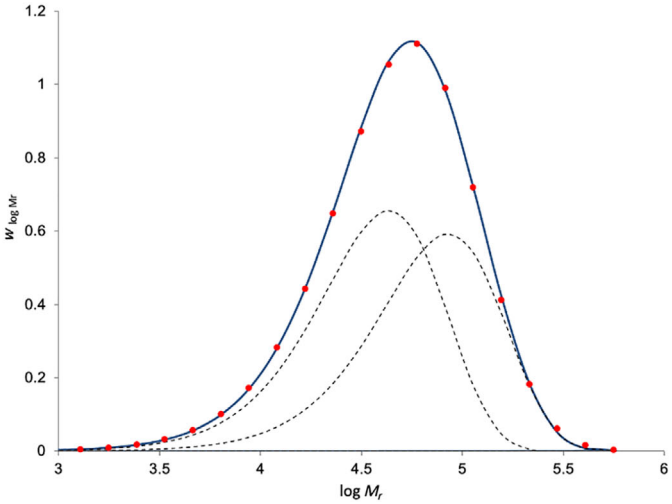

Site No.	M_n	m
1	22 000	0.53
2	43 000	0.47

FIGURE 13 Deconvolution of the broader molecular weight distribution (MWD) (red distribution, shown here as red dots) in Figure 12 using two Flory distributions. The continuous blue curve is the superposition of the two Flory distributions (interrupted lines).

ones measured for polyolefins made with supported metallocenes—but not the MWD of polyolefins produced with Ziegler–Natta catalysts, at least not if we assume that f_p and f_{t_H} follow normal distributions. (We could use distributions other than normal, but nature loves normal distributions; this is why I chose them for this thought experiment.) This isn't surprising, since Ziegler–Natta catalysts must have at least two different site types to explain bimodal TREF and CEF profiles for LLDPE resins and polypropylenes with different stereo- and regioregularities.

Can the MWD of these polyolefins be modelled as the superposition of two ratio distributions? Figure 14 answers this question in the affirmative. Two ratio distributions generate a broad MWD with $Đ = 4.2$, which is within the range of Ziegler–Natta polyolefins, supporting my hypothesis that this is an alternative way to model the broad MWDs made with multiple-site-type catalysts.

Figure 15 shows that the broad MWD in Figure 14 can be deconvoluted into five Flory distributions. Once again, we find ourselves in the same predicament: The classic MWD deconvolution method erroneously detects three additional Flory site types for an MWD formed by the superposition of two ratio distributions.

Where does this thought experiment leaves us? Both methods—deconvolution into Flory or ratio distributions—describe the digital MWD well. We cannot tell them apart. The two 'lenses' capture the same reality distinctly. We would need to fit the MWDs of several polyolefin samples made with the same catalyst under different polymerization conditions with both methods—and also likely compare different distributions for f_p and f_{t_H}—to find out which one would be more adequate. This investigation vastly exceeds the scope of this article.

If we are being pragmatic, we may prefer to deconvolute MWDs with Flory distributions: this method is easier to use, converges to unique solutions, and involves fewer assumptions. The ratio distribution method I proposed above is appealing because it reduces the number of site types by incorporating (indirectly) into the model effects caused by the support surface. But it requires that we decide which distributions to use in Equations (14) and (15)—they don't even have to be the same for f_p and f_{t_H}—and is likely to converge to multiple solutions. Ultimately, deciding which method you will select depends on what you want to do with your model. An effective olefin polymerization process simulator needs a microstructural model that can make accurate predictions. In this very practical sense, the model that fits the data more easily with fewer parameters and still achieves accurate predictions is the correct model. But if your intent is to use your model to probe the nature of coordination catalysts for olefin polymerization, it may be worth digging deeper and developing a model that can be correlated with the actual active site types (whatever these elusive entities may be) on these catalysts. For instance, it would be intriguing to use this model to shed light on how different support types and supporting methods affect the MWD of polyolefins made with a supported metallocene that behaves as single-site-type catalyst when unsupported.

The approach I am proposing here is, evidently, not restricted to modelling MWDs. It can be extended to CCDs by also expressing the reactivity ratios in the Stockmayer CCD components as ratio distributions

$$r_1 = \frac{k_{p_{11}}}{k_{p_{12}}}; r_2 = \frac{k_{p_{22}}}{k_{p_{21}}} \tag{20}$$

where the propagation rate constants also follow normal (or other) distributions

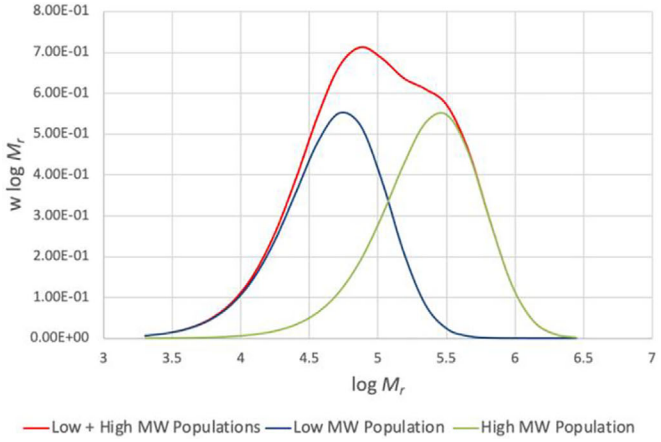

	Low MW Population	High MW Population	Low + High MW Populations
μ_{f_p}	1×10^5	1×10^6	
σ_{f_p}	2.5×10^4	2.6×10^5	
$\mu_{f_{tH}}$	100	200	
$\sigma_{f_{tH}}$	25	50	
M_n	29 000	140 000	48 000
M_w/M_n	2.2	2.4	4.2

FIGURE 14 Representation of a molecular weight distribution (MWD) as the superposition of two MWDs generated with Equation (19)

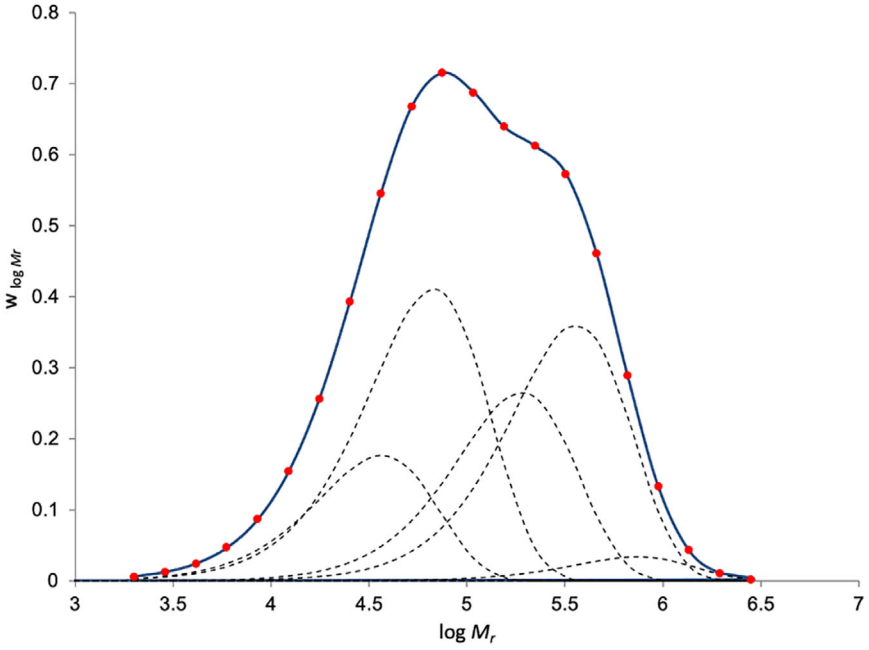

Site #	M_n	m
1	18 000	0.14
2	34 000	0.33
3	95 000	0.21
4	180 000	0.29
5	370 000	0.03

FIGURE 15 Deconvolution of the combined molecular weight distribution (MWD) (red distribution, shown here as red dots) in Figure 14 using five Flory distributions. The continuous blue curve is the superposition of the five Flory distributions (interrupted lines).

$$N\left(k_{p_{ij}}\right) = \frac{1}{\sigma_{k_{pij}}\sqrt{2\pi}} \exp\left[-\frac{1}{2}\left(\frac{k_{p_{ij}} - \mu_{k_{p11}}}{\sigma_{k_{p11}}}\right)^2\right] \quad (21)$$

This formulation would result in a distribution of values for the parameter β in Equations (4) and (6), allowing the deconvolution model to fit the experimental CCDs and joint MWD × CCDs with fewer Stockmayer distributions than in the classic approach.

4 | IN PRAISE OF SIMPLE SOLUTIONS

After reading this article, you may end up wondering whether I think that using deconvolution models—loaded with simplifying assumptions as they are—is worth the effort.

First, we need to comply with an extensive list of requirements—essentially discounting all effects that don't happen at the active site level, assuming steady-state conditions everywhere, and perfect polymer analysis results—before we can start our deconvolutions. Considering the confounding phenomena taking place at other scales in the reactor,[10] it may be hard—perhaps even impossible—to satisfy all of these requirements. In a recent article, we suggested that seven mathematical modelling levels were needed to completely describe olefin polymerization with coordination catalysts (Figure 16). Deconvolution models—as they are practiced today—are restricted to the two innermost levels: catalysis, where instantaneous distributions define the polymer microstructure, and polymerization kinetics.

We also need to decide which function describes the microstructural distributions made on each site type: Flory, Stockmayer, normal, log-normal, Wesslau, Lorenz, ratio, etc.? From the polymer analysis side, we need to neglect—or correct for—GPC peak broadening when measuring MWDs; for TREF, CEF, and CRYSTAF analysis, used in CCD deconvolution, we must ignore the influence of co-crystallization and crystallization dynamics. (HT-TGIC and HT-SGIC have problems of their own that I won't discuss here.) The deconvolution of TREF × GPC cross fractionation combines the previous two sets of limitations into a single one. GPC-IR deconvolution suffers from poor resolution for samples with low SCB frequencies. The list of limitations and simplifications may make you question the utility of these methods.

After reading this article, you may also realize that my question above was purely rhetorical. Of course, I think these methods are valuable, both as convenient models that quantify complex phenomena with a few parameters in polymerization process simulators and as conceptual lenses that let us probe into the nature of coordination catalysts for olefin polymerization. When properly used—and the qualification properly is essential here—these models will generate slightly different, albeit coherent answers. For instance, a narrowing of the MWD due to the addition of an electron donor to a catalyst may

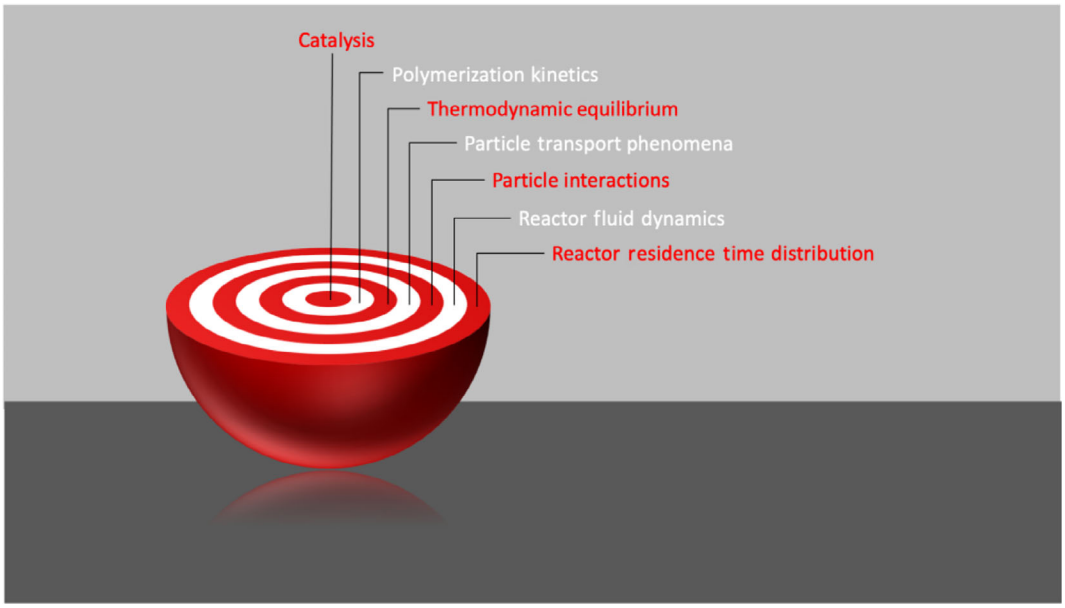

FIGURE 16 Conceptual mathematical modelling levels in olefin polymerization. Reproduced from Soares and McKenna[10]

be attributed to the selective poisoning of certain site types when using a Flory model, or to changes in the standard deviations of propagation and chain transfer frequencies when using a ratio distribution model. But both methods will let you quantify this effect, fit existing experimental data (the training set), predict the outcome of experiments at different conditions (the validation set), and—more importantly—design new experiments to test your model assumptions. If your model fails the test, you may modify it and try again. If the failure is irreparable, you may replace it with a new model based on a different set of premises; no matter the outcome, you will understand the nature of your polymerization system better with a model than without one. And it is likely that you may understand your system better with the simplest possible model. Complex models with many simultaneous algebraic and differential equations may be powerful—although sometimes they are just dazzling ways to hide our lack of understanding—but when you can describe a process with a few simple equations, you know you have peered into its essence.

Sometime ago, I came across a quote attributed to J. B. S. Haldane, 'An ounce of algebra is worth a ton of verbal argument,' that resonated with me. According to John Maynard Smith, '[Haldane] did have a genius for taking a complex biological problem and simplifying it to the stage at which it could be posed in mathematical form, without at the same time distorting it out of recognition.'[167] I think that all of us can learn a lot from Haldane's approach to modelling complex systems.

5 | POSTSCRIPT

You doubtless noticed that I wrote this article avoiding the stuffy language that you sadly find in most scientific communications. (Take a look at how Giulio Natta wrote his outstanding paper in 1959,[9] without any of the nonsense that infects the technical literature today.) I chose this style to honour Archie, who was among the least pretentious persons I have ever met. In fact, he often told me that he was only a process engineer. Among so many things, he taught me that the concepts we discuss in our articles may be complex, but how we discuss them should never be. It's no wonder he was such a wonderful expert witness.

The first article I wrote in my PhD thesis was about temperature rising elution fractionation (TREF).[168] The first draft—unsurprisingly for an aspiring academic tainted by the drivel he was reading in the literature—was boring, pompous, and constrained by many of the vices that plague formal scientific writing. I will never forget Archie returning it to me and telling me to rewrite it in a way that the readers—and he—would be motivated to learn about my new findings. He told me, 'you are the expert on TREF. You can write a more interesting paper,' which unquestionably was a very lax use of the word expert as it applied to me at that time. But this was Archie at his best, always willing to help his students uncover their abilities. With his incentive, I wrote a second draft that Archie did like—he told me it was an excellent second draft—but to this day I am not sure whether he meant it or just wanted to cheer me up.

Archie's lesson on clear writing—and clear thinking—has been a beacon throughout my whole career. I hope you like this article too, Archie.

NOMENCLATURE

$[C^*]$	concentration of active sites
$Đ$	dispersity
f_p	monomer propagation frequency
f_{t_i}	chain transfer frequency
$F_Z(\tau)$	ratio distribution for τ, Equations (16) and (17)
F_1	molar fraction of ethylene in a copolymer chain
$\overline{F}_1$	average fraction of ethylene in the copolymer population
k_{a_i}	activation rate constant for site type i
k_{d_i}	deactivation rate constant for site type i
k_{p_i}	propagation rate constant for site type i
$k_{p_{ij}}$	copolymerization rate constant for monomer i and comonomer j
k_{t_β}	rate constant for β-hydride elimination
k_{t_H}	rate constant for chain transfer to hydrogen
k_{t_M}	rate constant for chain transfer to monomer
m_i	mass fraction of polymer made by site type i
$[M]$	monomer concentration
$\overline{M}$	average molar mass of the repeating unit
M_n	number average molecular weight
M_r	molar mass of a polymer chain of length r
M_w	weight average molecular weight
n	number of active site types
$N\left(f_p\right)$	normal distribution for f_p, Equation (14)
$N\left(f_{t_H}\right)$	normal distribution for f_{t_H}, Equation (15)
r_1, r_2	reactivity ratios for monomer 1 (ethylene) and 2 (1-olefin)
R_{p_i}	monomer propagation rate for site type i, Equation (9)
t	polymerization time
T	temperature
T_{c_i}	CRYSTAF crystallization temperature
T_{e_i}	TREF elution temperature
w_{F_1}	chemical composition component of the Stockmayer distribution, Equation (4)
$w_{\log M_r}$	Flory most probable distribution in log scale, Equation (1); molecular weight distribution, Equation (19)
$W^{exp}_{\log M_r}$	experimental MWD
$w_{\log M_r, F_1}$	Stockmayer bivariate distribution, Equation (6)
Y_p	polymer yield

Greek letters

β	Stockmayer distribution parameter, Equation (5)
$\Theta\left(f_{t_i}\right)$	distribution for f_{t_i}, Equation (8)
λ	normalization constant for Flory most probable distribution, Equation (1)
μ_{f_p}	mean value for f_p, Equation (14)
$\mu_{f_{tH}}$	mean value for f_{t_H}, Equation (15)
$\Xi\left(f_p\right)$	distribution for f_p, Equation (8)
σ	standard deviation
σ_{f_p}	standard deviation for f_p, Equation (14)
$\sigma_{f_{tH}}$	standard deviation for f_{t_H}, Equation (15)
τ	ratio of total chain transfer to propagation rate, Equation (2)
$\Phi(\tau)$	distribution for τ, Equation (8)

Acronyms

CCD	chemical composition distribution
CEF	crystallization elution fractionation
CFC	cross fractionation
CRYSTAF	crystallization analysis fractionation
CSLD	comonomer sequence length distribution
FTIR	Fourier-transform infrared
GPC	gel permeation chromatography
IDEM	integrated deconvolution estimation model
HDPE	high-density polyethylene
HT-SGIC	high-temperature solvent gradient interaction chromatography
HT-TGIC	high-temperature thermal gradient interaction chromatography
IR	infrared
LCB	long chain branch
LLDPE	linear low-density polyethylene
MWD	molecular weight distribution
SCB	short chain branch
TREF	temperature rising elution fractionation

AUTHOR CONTRIBUTIONS

João B. P. Soares: Conceptualization; formal analysis; methodology; writing – original draft; writing – review and editing.

PEER REVIEW

The peer review history for this article is available at https://publons.com/publon/10.1002/cjce.24833.

DATA AVAILABILITY STATEMENT

Data available on request from the authors.

ORCID

João B. P. Soares https://orcid.org/0000-0001-8017-143X

REFERENCES

[1] P. J. Flory, *J. Am. Chem. Soc.* **1940**, *62*, 1561.
[2] P. J. Flory, *J. Am. Chem. Soc.* **1942**, *64*, 2205.
[3] P. J. Flory, *J. Chem. Phys.* **1944**, *12*, 425.

[4] P. J. Flory, *Principles of Polymer Chemistry*, Cornell University Press, New York **1953**.
[5] G. V. Schulz, *Zeitschrift für Physikalische Chemie* **1939**, *B43*, 25.
[6] J. B. P. Soares, A. E. Hamielec, *Polym. React. Eng.* **1995**, *3*, 261.
[7] H. Fogler, *Elements of Chemical Reaction Engineering*, 6th ed., Pearson, New York **2020**.
[8] C. Vogt, B. M. Weckhuysen, *Nat. Rev. Chem.* **2022**, *6*, 89.
[9] G. Natta, *J. Polym. Sci.* **1959**, *34*, 21.
[10] J. B. P. Soares, T. F. L. McKenna, *Can. J. Chem. Eng.* **2022**, *100*, 2432.
[11] F. W. Karasek, R. J. Laub, E. De Decker, *J. Chromatogr.* **1974**, *93*, 123.
[12] R. A. Vaidya, R. D. Hester, *J. Chromatogr.* **1984**, *287*, 231.
[13] R. F. Lacey, *Anal. Chem.* **1986**, *58*, 1404.
[14] P. B. Crilly, *J. Chemom.* **1987**, *1*, 79.
[15] A. N. Papas, *Anal. Chem.* **1990**, *62*, 234.
[16] C. P. Cai, N. S. Wu, *Chromatographia* **1991**, *31*, 595.
[17] A. Gergely, P. Horváth, B. Noszál, *J. Chromatogr. Sci.* **2000**, *38*, 425.
[18] V. B. Di Marco, G. G. Bombi, *J. Chromatogr. A* **2001**, *931*, 1.
[19] G. Vivó-Truyols, J. R. Torres-Lapasió, A. M. van Nederkassel, Y. Vander Heyden, D. L. Massart, *J. Chromatogr. A* **2005**, *1096*, 146.
[20] V. V. Vickroy, H. Schneider, R. F. Abbott, *J. Appl. Polym. Sci.* **1993**, *50*, 551.
[21] W. H. Stockmayer, *J. Chem. Phys.* **1945**, *13*, 199.
[22] J. B. P. Soares, A. E. Hamielec, *Macromol. Theory Simul.* **1995**, *4*, 305.
[23] J. B. P. Soares, A. E. Hamielec, *Polymer* **1995**, *36*, 2257.
[24] D. Beigzadeh, J. B. P. Soares, T. A. Duever, *J. Appl. Polym. Sci.* **2001**, *80*, 2200.
[25] J. B. P. Soares, B. Monrabal, J. Blanco, J. Nieto, *Macromol. Chem. Phys.* **1917**, *1998*, 199.
[26] S. Anantawaraskul, J. B. P. Soares, P. M. Wood-Adams, *Polymer* **2003**, *44*, 2393.
[27] S. Anantawaraskul, J. B. P. Soares, P. M. Wood-Adams, *J. Polym. Sci., Part B: Polym. Phys.* **2003**, *41*, 1762.
[28] S. Anantawaraskul, J. B. P. Soares, P. M. Wood-Adams, *Macromol. Chem. Phys.* **2004**, *205*, 771.
[29] K. Suriya, S. Anantawaraskul, J. B. P. Soares, *J. Polym. Sci., Part B: Polym. Phys.* **2011**, *49*, 678.
[30] S. Anantawaraskul, J. B. P. Soares, P. Jirachaithorn, N. Sornprom, J. Limtrajul, *J. Polym. Sci., Part B: Polym. Phys.* **2006**, *44*, 2749.
[31] S. Anantawaraskul, J. B. P. Soares, P. Jirachaithorn, *Macromol. Symp.* **2007**, *257*, 94.
[32] S. Anantawaraskul, P. Jirachaithorn, J. B. P. Soares, J. Limtrakul, *J. Polym. Sci., Part B: Polym. Phys.* **2007**, *45*, 1010.
[33] S. Anantawaraskul, P. Somnukguandee, J. B. P. Soares, J. Limtrakul, *J. Polym. Sci., Part B: Polym. Phys.* **2009**, *47*, 866.
[34] N. Chokputtanawuttilerd, S. Anantawaraskul, A. A. Alghyamah, J. B. P. Soares, *Macromol. Chem. Phys.* **2013**, *214*, 2591.
[35] N. Chokputtanawuttilerd, S. Anantawaraskul, J. B. P. Soares, *Macromol. Symp.* **2013**, *330*, 132.
[36] N. Inwong, S. Anantawaraskul, J. B. P. Soares, A. Al-Khazaal, *Macromol. Symp.* **2015**, *354*, 361.
[37] N. Chokputtanawuttilerd, N. Inwong, S. Anantawaraskul, J. B. P. Soares, *Macromol. Chem. Phys.* **2015**, *216*, 621.
[38] J. B. P. Soares, A. E. Hamielec, *Macromol. Theory Simul.* **1996**, *5*, 547.
[39] J. B. P. Soares, A. E. Hamielec, *Macromol. Theory Simul.* **1997**, *6*, 591.
[40] J. B. P. Soares, *Macromol. Mater. Eng.* **2004**, *289*, 70.
[41] A. Albeladi, J. B. P. Soares, S. Mehdiabadi, *Macromol. React. Eng.* **2018**, *13*, 1800059.
[42] Y. V. Kissin, *Makromol. Chem., Macromol. Symp.* **1993**, *66*, 83.
[43] E. Broyer, R. F. Abbott, in *Computer Applications in Applied Polymer Science, ACS Symposium Series* (Ed: T. Provder), American Chemical Society, Washington, DC **1982**, p. 45.
[44] Y. V. Kissin, *J. Polym. Sci., Part A: Polym. Chem.* **1995**, *33*, 227.
[45] H. Wesslau, *Makromol. Chem.* **1956**, *20*, 111.
[46] H. Wesslau, *Makromol. Chem.* **1958**, *26*, 102.
[47] W. C. Taylor, L. H. Huang, *J. Polym. Sci., Polym. Lett. Ed.* **1963**, *1*, 157.
[48] T. Keii, *Macromol. Theory Simul.* **1995**, *4*, 947.
[49] J. B. P. Soares, *Polym. React. Eng.* **1998**, *6*, 225.
[50] G. Maschio, C. Bruni, L. De Tullio, F. Ciardelli, *Macromol. Chem. Phys.* **1998**, *199*, 415.
[51] Y. V. Kissin, R. Ohnishi, T. Konakazawa, *Macromol. Chem. Phys.* **2004**, *205*, 284.
[52] X. Jiang, Y. P. Chen, Z. Q. Fan, Q. Wang, Z. S. Fu, J. T. Xu, *J. Mol. Catal. A: Chem.* **2005**, *235*, 209.
[53] F. M. Silva, P. A. Melo, M. Nele, E. L. Lima, J. C. Pinto, *Macromol. Mater. Eng.* **2006**, *219*, 540.
[54] L. T. Zhang, Z. Q. Fan, Z. S. Fu, *Chin. J. Polym. Sci.* **2008**, *26*, 605.
[55] F. Machado, E. L. Lima, J. C. Pinto, T. F. McKenna, *Eur. Polym. J.* **2008**, *44*, 1102.
[56] F. Machado, E. L. Lima, J. C. Pinto, T. F. McKenna, *Eur. Polym. J.* **2008**, *44*, 1130.
[57] A. T. M. Kamrul Hasan, Y. Fang, B. Liu, M. Terano, *Polymer* **2010**, *51*, 3627.
[58] S. T. Tu, J. Q. Lou, Z. S. Fu, Z. Q. Fan, *e-Polymers* **2011**, *11*, 1.
[59] X. Jiang, H. Wang, X. Tian, Y. Yang, Z. Fan, *Ind. Eng. Chem. Res.* **2011**, *50*, 259.
[60] M. Nikolaeva, M. Matsko, T. Mikenas, V. Zakharov, *J. Appl. Polym. Sci.* **2014**, *131*, 40658.
[61] S. Hakim, M. Nekoomanesh, A. Shahrokhinia, *Polym. Sci., Ser. A* **2015**, *57*, 573.
[62] P. Li, S. Tu, T. Xu, Z. Fu, Z. Fan, *J. Appl. Polym. Sci.* **2015**, *132*, 41689.
[63] Q. Zhou, A. Wang, H. Li, Z. Luo, T. Zheng, L. Zhang, Y. Hu, *RSC Adv.* **2016**, *6*, 75023.
[64] Q. Zhao, H. Xu, A. Wang, Z. Ma, H. Li, L. Zhang, Y. Hu, *J. Appl. Polym. Sci.* **2017**, *134*, 44704.
[65] S. Hakim, M. Nekoomanesh, A. Shahrokhinia, *Polyolefins J.* **2019**, *6*, 139.
[66] N. G. Hamedani, H. Arabi, F. Poorsank, *New J. Chem.* **2020**, *44*, 1578.
[67] Y. P. Chen, Z. Q. Fan, J. H. Liao, S. Q. Liao, *J. Appl. Polym. Sci.* **2006**, *102*, 1768.
[68] D. E. Thompson, K. B. McAuley, P. J. McLellan, *Macromol. React. Eng.* **2007**, *1*, 264.
[69] D. E. Thompson, K. B. McAuley, P. J. McLellan, *Macromol. React. Eng.* **2007**, *1*, 523.

[70] M. A. Matsko, L. G. Echevskaya, V. A. Zakharov, M. I. Nikolaeva, T. B. Mikenas, M. P. Vanina, *Macromol. Symp.* **2009**, *282*, 157.

[71] M. I. Nikolaeva, T. B. Mikenas, M. A. Matkso, L. G. Echevskaya, V. A. Zakharov, *J. Appl. Polym. Sci.* **2009**, *115*, 2432.

[72] L. Wang, M. Yang, H. Ren, W. Cui, B. Lui, W. Yan, *Macromol. Res.* **2010**, *18*, 94.

[73] M. I. Nikolaeva, T. B. Mikenas, M. A. Matkso, L. G. Echevskaya, V. A. Zakharov, *J. Appl. Polym. Sci.* **2011**, *122*, 3092.

[74] M. I. Nikolaeva, T. B. Mikenas, M. A. Matkso, L. G. Echevskaya, V. A. Zakharov, *J. Appl. Polym. Sci.* **2012**, *125*, 2034.

[75] M. I. Nikolaeva, T. B. Mikenas, M. A. Matkso, L. G. Echevskaya, V. A. Zakharov, *J. Appl. Polym. Sci.* **2012**, *125*, 2042.

[76] C. de Lemos, F. Franceschini, C. Radtke, J. H. Z. dos Santos, C. R. Wolf, *Appl. Catal., A* **2012**, *423-424*, 69.

[77] T. Xu, H. Yang, Z. Fu, Z. Fan, *J. Organomet. Chem.* **2015**, *785*, 328.

[78] B. Jiang, Y. Weng, S. Zhang, Z. Zhang, Z. Fu, Z. Fan, *J. Catal.* **2018**, *360*, 57.

[79] S. M. G. Zarand, A. Safinejad, *Polyolefins J.* **2020**, *7*, 121.

[80] M. Matsko, M. I. Nikolaeva, V. A. Zakharov, *J. Appl. Polym. Sci.* **2021**, *138*, e50256.

[81] M. Masoori, R. Rashedi, A. Sepahi, M. H. Jandaghian, E. Nikzinat, S. Houshmandmoayed, *J. Polym. Res.* **2022**, *29*, 1.

[82] M. McDaniel, *Appl. Catal., A* **2017**, *542*, 392.

[83] B. Liu, Z. Tian, N. Zhao, Z. Liu, B. Liu, *Ind. Eng. Chem. Res.* **2017**, *56*, 6164.

[84] Y. Liu, R. Zhang, H. Ren, Y. Liu, S. Ling, H. Zhang, B. Liu, R. Cheng, *Macromol. Chem. Phys.* **2020**, *221*, 2000010.

[85] Z. Q. Fan, L. X. Feng, S. L. Yang, *J. Polym. Sci., Part A: Polym. Chem.* **1996**, *34*, 3329.

[86] X. Jiang, X. Tian, Z. Fan, K. Fang, Z. Fu, J. Xu, Q. Wang, *J. Mol. Catal. A: Chem.* **2007**, *275*, 72.

[87] L. Echevskaya, M. Matsko, M. Nikolaeva, S. Sergeev, V. Zakharov, *Macromol. React. Eng.* **2014**, *8*, 666.

[88] H. Yang, L. Zhang, D. Zang, Z. Fu, Z. Fan, *Catal. Commun.* **2015**, *62*, 104.

[89] F. Nouri-Ahangarani, M. Nekoomanesh-Haghighi, S. A. Mirmohammadi, N. Bahri-Laleh, *Polyolefins J.* **2017**, *4*, 254.

[90] X. Dong, L. Zhang, Z. Liu, M. Yang, Z. Duan, K. Hou, B. Liu, I. Kim, *J. Appl. Polym. Sci.* **2014**, *131*, 40758.

[91] W. Zheng, Y. Zhao, M. Han, C. Zhou, A. He, *Polymer* **2021**, *228*, 123925.

[92] V. Matos, A. G. Mattos Neto, J. C. Pinto, *J. Appl. Polym. Sci.* **2001**, *79*, 2076.

[93] V. Matos, A. G. Mattos Neto, J. C. Pinto, *J. Appl. Polym. Sci.* **2002**, *86*, 3226.

[94] V. Matos, M. Moreira, A. G. Mattos Neto, M. Nele, P. A. Melo, J. C. Pinto, *Macromol. React. Eng.* **2007**, *1*, 137.

[95] J. B. P. Soares, J. D. Kim, G. L. Rempel, *Ind. Eng. Chem. Res.* **1997**, *36*, 1144.

[96] R. Leino, H. J. G. Luttikhedde, P. Lehmus, C. E. Wilén, R. Sjöholm, A. Lehtonen, J. V. Seppälä, J. H. Näsman, *J. Organomet. Chem.* **1998**, *559*, 65.

[97] L. D'Agnillo, J. B. P. Soares, A. Penlidis, *J. Polym. Sci., Part A: Polym. Chem.* **1998**, *36*, 831.

[98] Q. Wang, J. Weng, L. Xu, Z. Fan, L. Feng, *Polymer* **1999**, *40*, 1863.

[99] J. B. P. Soares, J. D. Kim, *J. Polym. Sci., Part A: Polym. Chem.* **2000**, *38*, 1408.

[100] A. Tynys, T. Saarinen, M. Bartke, B. Löfgren, *Polymer* **2007**, *48*, 1893.

[101] A. A. Barabanov, N. V. Semikolenova, M. A. Matsko, L. G. Echevskaya, V. A. Zakharov, *Polymer* **2010**, *51*, 3354.

[102] H. Hamaki, N. Tadeka, M. Nabika, N. Tokitoh, *Macromolecules* **2012**, *45*, 1758.

[103] Y. Guo, F. He, Z. Zhang, A. Khan, Z. Fu, J. Xu, Z. Fan, *J. Organomet. Chem.* **2016**, *808*, 109.

[104] A. Atashrouz, M. Rahmani, B. Nasernejad, Z. Balzade, *Mater. Chem. Phys.* **2020**, *255*, 123466.

[105] A. Ali, N. Muhammad, S. Hussain, M. I. Jamil, A. Uddin, T. Aziz, M. K. Tufail, Y. Guo, T. Wei, G. Rasool, Z. Fan, L. Guo, *Polymer* **2021**, *13*, 268.

[106] S. Mehdiabadi, O. Lhost, A. Vantomme, J. B. P. Soares, *Ind. Eng. Chem. Res.* **2021**, *60*, 9739.

[107] S. Mehdiabadi, O. Lhost, A. Vantomme, J. B. P. Soares, *Macromol. React. Eng.* **2021**, *15*, 2100041.

[108] N. P. Khare, B. Lucas, K. C. Seavey, Y. A. Liu, A. Sirohi, S. Ramanathan, S. Lingard, Y. Song, C. C. Chen, *Ind. Eng. Chem. Res.* **2004**, *43*, 884.

[109] Z. H. Luo, P. L. Su, D. P. Shi, Z. W. Zheng, *Chem. Eng. J.* **2009**, *149*, 370.

[110] N. Sharma, Y. A. Liu, *Ind. Eng. Chem. Res.* **2019**, *58*, 14209.

[111] J. B. P. Soares, T. Shouli, A. E. Hamielec, *Polym. React. Eng.* **1997**, *5*, 25.

[112] D. C. Pernusch, G. Spiegel, C. Paulik, W. Hofer, *Macromol. React. Eng.* **2022**, *16*, 21000020.

[113] M. Fortuny, M. Nele, P. A. Melo, J. C. Pinto, *Macromol. Theory Simul.* **2004**, *13*, 355.

[114] G. Singh, S. Kaur, D. G. Naik, V. K. Gupta, *J. Appl. Polym. Sci.* **2010**, *117*, 3379.

[115] H. R. Patil, S. Karthikeyan, V. Kote, P. Sengupta, P. Samanta, P. Kadam, N. Venkateswaran, V. K. Gupta, *Polym. Bull.* **2022**, *79*, 1.

[116] J. B. P. Soares, *Chem. Eng. Sci.* **2001**, *56*, 4131.

[117] A. A. da Silva Filho, G. B. de Galland, J. B. P. Soares, *Macromol. Chem. Phys.* **2000**, *201*, 1226.

[118] Y. V. Kissin, H. A. Fruitwala, *J. Appl. Polym. Sci.* **2007**, *106*, 3872.

[119] Y. V. Kissin, F. M. Mirabella, C. C. Meverden, *J. Polym. Sci., Part A: Polym. Chem.* **2005**, *43*, 4351.

[120] Q. Wang, N. Murayama, B. Liu, M. Terano, *Macromol. Chem. Phys.* **2005**, *206*, 961.

[121] J. B. P. Soares, A. E. Hamielec, *Macromol. React. Eng.* **2008**, *2*, 115.

[122] J. B. P. Soares, A. E. Hamielec, *Macromol. React. Eng.* **2007**, *1*, 53.

[123] A. A. Alghyamah, J. B. P. Soares, *Macromol. Rapid Commun.* **2009**, *30*, 384.

[124] A. A. Alghyamah, J. B. P. Soares, *Macromol. Symp.* **2009**, *285*, 81.

[125] S. Anantawaraskul, W. Bongsontia, J. B. P. Soares, *Macromol. Symp.* **2009**, *282*, 167.

[126] U. Nanthapoolsub, S. Anantawaraskul, K. Saengkhamkhom, *Macromol. Symp.* **2013**, *330*, 142.

[127] S. Anantawaraskul, W. Bongsontia, J. B. P. Soares, *Macromol. React. Eng.* **2011**, *5*, 549.
[128] C. Hornchaiya, S. Anantawaraskul, J. B. P. Soares, S. Mehdiabadi, *Macromol. Chem. Phys.* **2019**, *220*, 1800522.
[129] T. Chayrattanoroj, S. Anantawaraskul, *Macromol. Symp.* **2020**, *390*, 1900023.
[130] K. Khayanying, S. Anantawaraskul, *Macromol. Symp.* **2020**, *390*, 1900024.
[131] J. B. P. Soares, R. F. Abbott, J. N. Willis, X. Liu, *Macromol. Chem. Phys.* **1996**, *197*, 3383.
[132] A. Ortin, J. Montesinos, E. López, P. del Hierro, B. Monrabal, J. R. Torres-Lapasió, M. C. García-Álvarez-Coque, *Macromol. Symp.* **2013**, *330*, 63.
[133] J. B. P. Soares, T. F. McKenna, *Polyolefin Reaction Engineering*, Wiley-VCH, Weinheim, Germany **2012**.
[134] A. Faldi, J. B. P. Soares, *Polymer* **2001**, *42*, 3057.
[135] K. Chen, S. Mehdiabadi, B. Liu, J. B. P. Soares, *Macromol. React. Eng.* **2016**, *10*, 206.
[136] F. Pérez Valencia, J. B. P. Soares, *Macromol. Symp.* **2007**, *259*, 110.
[137] Z. Tian, K. R. Chen, B. P. Liu, N. Luo, W. L. Du, F. Qian, *Chem. Eng. Sci.* **2015**, *130*, 41.
[138] H. H. Feng, X. Chen, X. P. Gu, L. F. Feng, D. F. Wang, G. X. Yang, Y. X. Gao, C. L. Zhang, G. H. Hu, *Chem. Eng. Sci.* **2022**, *261*, 117952.
[139] L. Göpperl, D. Pernuch, J. Schwarz, C. Paulik, *Macromol. React. Eng.* **2022**, *16*, 21000042.
[140] M. A. Al-Saleh, J. B. P. Soares, T. A. Duever, *Macromol. React. Eng.* **2010**, *4*, 578.
[141] M. A. Al-Saleh, J. B. P. Soares, T. A. Duever, *Macromol. React. Eng.* **2011**, *5*, 587.
[142] M. A. Al-Saleh, J. B. P. Soares, T. A. Duever, *Macromol. React. Eng.* **2012**, *6*, 189.
[143] X. P. Cheng, L. F. Feng, X. P. Gu, X. Chen, Z. G. Liu, K. B. McAuley, *AIChE J.* **2020**, *66*(1), e16784.
[144] Y. V. Kissin, *Macromol. Symp.* **1995**, *89*, 113.
[145] Y. V. Kissin, R. I. Mink, T. E. Nowlin, *J. Polym. Sci.: Part A: Polym. Chem.* **1999**, *37*, 4255.
[146] Y. V. Kissin, R. I. Mink, T. E. Nowlin, A. J. Brandolini, *Top. Catal.* **1999**, *7*, 69.
[147] Y. V. Kissin, *J. Polym. Sci., Part A: Polym. Chem.* **2003**, *41*, 1745.
[148] M. Ahmadi, M. Nekoomanesh, H. Arabi, *Macromol. React. Eng.* **2010**, *4*, 135.
[149] H. Yang, L. Zhang, Z. Fu, Z. Fan, *J. Appl. Polym. Sci.* **2015**, *132*, 41264.
[150] K. Chen, S. Mehdiabadi, B. Liu, J. B. P. Soares, *Macromol. React. Eng.* **2016**, *10*, 551.
[151] T. Charoenpanich, S. Anantawaraskul, J. B. P. Soares, P. Wongmahasirikun, S. Shiohara, *Macromol. React. Eng.* **2022**, *16*, 2200027.
[152] A. Alshaiban, J. B. P. Soares, *Macromol. React. Eng.* **2012**, *6-7*, 265.
[153] K. Chen, B. Liu, J. B. P. Soares, *Macromol. React. Eng.* **2016**, *10*, 463.
[154] T. F. McKenna, J. B. P. Soares, *Chem. Eng. Sci.* **2001**, *56*, 3931.
[155] Y. Zhou, A. Alizadeh, B. Liu, J. B. P. Soares, *Macromol. React. Eng.* **2020**, *14*, 200043.
[156] B. Liu, B. Liu, J. B. P. Soares, *Macromol. React. Eng.* **2018**, *12*, 1800054.
[157] B. Liu, J. Romero, B. Liu, J. B. P. Soares, *Macromol. React. Eng.* **2018**, *12*, 1800051.
[158] A. Ortin, B. Monrabal, J. Sancho-Tello, *Macromol. Symp.* **2007**, *257*, 13.
[159] C. C. Tso, P. J. DesLauriers, *Polymer* **2004**, *45*, 2657.
[160] H. N. Cheng, *Computer Applications in Applied Polymer Science II*, American Chemical Society, Washington, DC **1989**, p. 174 Ch. 17.
[161] H. N. Cheng, *Polym. Bull.* **1990**, *23*, 589.
[162] H. N. Cheng, *New Advances in Polyolefins*, Plenum Press, New York **1993**, p. 15.
[163] H. N. Cheng, *Polym. Bull.* **1991**, *26*, 325.
[164] H. N. Cheng, *Macromolecules* **1991**, *24*, 4813.
[165] V. Touloupidis, A. Albretch, J. B. P. Soares, *Macromol. React. Eng.* **2018**, *12*, 1700056.
[166] A. Oliveira, T. Oliveira, A. Seijas-Macías, *AIP Conf. Proc.* **2015**, *1648*, 840005.
[167] J. M. Smith, *Nature* **1965**, *4981*, 239.
[168] J. B. P. Soares, A. E. Hamielec, *Polymer* **1995**, *36*, 1639.
[169] S. Mehdiabadi, J. B. P. Soares, *Macromolecules* **2012**, *45*, 1777.

How to cite this article: J. B. P. Soares, *Can. J. Chem. Eng.* **2023**, *101*(9), 4955. https://doi.org/10.1002/cjce.24833

APPENDIX A

The parameter τ in Flory most probable distribution is more commonly defined as the ratio of all chain transfer rates to the propagation rate

$$\tau = \frac{\sum R_{t_i}}{R_p} \tag{A.1}$$

The propagation rate of olefins with most coordination catalysts is given by the equation

$$R_p = k_p[M][C^*] \tag{A.2}$$

where k_p is the propagation rate constant, $[M]$ is the monomer concentration at the active site, and $[C^*]$ is the concentration of active sites. Since k_p is given in units of $\mathrm{L \cdot mol^{-1} \cdot s^{-1}}$, the product $f_p = k_p[M]$ is the frequency of monomer insertion in the growing polymer chains (propagation frequency).

$$R_p = f_p[C^*] \tag{A.3}$$

Similarly, most common chain transfer rates can also be expressed as frequencies

$$R_{t_M} = k_{t_M}[M][C^*] = f_{t_M}[C^*] \tag{A.4}$$

$$R_{t_H} = k_{t_H}[H][C^*] = f_{t_H}[C^*] \quad (A.5)$$

$$R_{t_\beta} = k_{t_\beta}[C^*] = f_{t_\beta}[C^*] \quad (A.6)$$

where the subscripts M,H, and β stand for transfer to monomer, transfer to hydrogen, and β-hydride elimination, respectively.

When we substitute Equations (A.3) to (A.6) in Equation (A.1), we obtain the definition of τ as a ratio of frequencies

$$\tau = \tau = \frac{\sum f_{t_i}}{f_p} = \frac{f_{t_M} + f_{t_H} + f_{t_\beta}}{f_p} \quad (A.7)$$

At first sight, the definitions of τ according to Equations (A.1) or (A.7) look equivalent—and you may feel that insisting that they aren't is merely academic nitpicking—but Equation (A.7) is more general because it doesn't depend on the functional forms of the rate laws for propagation and chain transfer. The rate laws expressed in Equations (A.2) and (A.4) to (A.6) cannot fit all polymerization rates measured experimentally for olefin polymerization with coordination catalysts. For instance, monomer concentration orders different from one have been reported for ethylene propagation with some catalysts.[169]

$$R_p = k_p[M]^n[C^*]\ n \neq 1 \quad (A.8)$$

A slightly different form of Equation (A.1) needs to be used in these cases, but Equation (A.7) or Equation (2) remains the same, since we only need to redefine the propagation frequency as

$$f_p = k_p[M]^n \quad (A.9)$$

As an additional advantage, functions that quantify f_p for homopolymerization and copolymerization have the same form.[10] Frequencies allow for a more general treatment and are easier to compare among reactions of different orders. Besides, the magnitude of a frequency has an intuitive feel ($1\ s^{-1}$ vs. $100\ s^{-1}$), which is lacking in the magnitude of a kinetic rate constant ($2\ L \cdot mol^{-1} \cdot s^{-1}$ vs. $200\ L \cdot mol^{-1} \cdot s^{-1}$).